## General Disclaimer

## One or more of the Following Statements may affect this Document

- This document has been reproduced from the best copy furnished by the organizational source. It is being released in the interest of making available as much information as possible.

- This document may contain data, which exceeds the sheet parameters. It was furnished in this condition by the organizational source and is the best copy available.

- This document may contain tone-on-tone or color graphs, charts and/or pictures, which have been reproduced in black and white.

- This document is paginated as submitted by the original source.

- Portions of this document are not fully legible due to the historical nature of some of the material. However, it is the best reproduction available from the original submission.

Produced by the NASA Center for Aerospace Information (CASI)

JPL PUBLICATION 82-56

(NASA-CR-169264) LIDAR AND ACCOUSTICS APPLICATIONS TO OCEAN PRODUCTIVITY (Jet Propulsion Lab.) 73 p HC A04/MF A01 CSCL 08C

N82-31884

Unclas G3/48 28794

# LIDAR and Acoustics Applications to Ocean Productivity

**Donald J. Collins**


June 1, 1982

National Aeronautics and
Space Administration

**Jet Propulsion Laboratory**
California Institute of Technology
Pasadena, California

JPL PUBLICATION 82-56

# LIDAR and Acoustics Applications to Ocean Productivity

**Donald J. Collins**

June 1, 1982

National Aeronautics and
Space Administration

**Jet Propulsion Laboratory**
California Institute of Technology
Pasadena, California

The research described in this publication was carried out by the Jet Propulsion Laboratory, California Institute of Technology, under contract with the National Aeronautics and Space Administration.

## FOREWORD

The National Aeronautics and Space Administration, through its charter to explore the planets and to assess the Earth's resources, has developed the technology and the expertise for the deployment of instrumentation capable of the remote measurement of global distributions of biologically important quantities. This preeminence in the use of space for the remote, near-synoptic measurement of ecological variables is important in the development of global ecological models and introduces the prospect for significant advances in physical and biological oceanography.

The measurement of physical variables and processes using the instruments on Seasat-1, and the measurement of biological variables and processes using the Coastal Zone Color Scanner on Nimbus-7, has encouraged interdisciplinary investigations at scientific institutions world-wide. This report summarizes the results of one effort to develop and apply the technology of the remote scientific measurement of physical variables to the study of the distributions and interactions of the lowest orders in the food chain in the world's oceans.

## ACKNOWLEDGMENTS

The author gratefully acknowledges the substantial contributions to the scientific rationale provided by the NASA ad hoc LIDAR Science Committee under the chairmanship of Dr. John Steele of the Woods Hole Oceanographic Institution. The members of that committee are:

Kendall Carder - University of South Florida
Donald Collins - Jet Propulsion Laboratory
Kenneth Denman - Institute of Ocean Sciences
Richard Eppley - Scripps Institution of Oceanography
Wayne Esaias - NASA Langley Research Center
Loren Haury - Scripps Institution of Oceanography
Michael Mullin - Scripps Institution of Oceanography
Trevor Platt - Bedford Institute of Oceanography
John Steele - Woods Hole Oceanographic Institution

The author would also like to acknowledge the participation in this study of Dr. Dale Kiefer and Dr. Richard Pieper of the University of Southern California and of Dr. Raymond Smith of the University of California at Santa Barbara, and a critical review by Dr. Mark Abbott of the Institute of Ocean Sciences at Patricia Bay, British Columbia. The NASA OSSA Program Manager was Dr. Kendall Carder.

The discussions of technology presented in this report are the results of the work of a team assembled at the Jet Propulsion Laboratory. Those who participated in this effort include:

James Breckinridge
Kent Frewing
Richard Heyser
Nathan Jacobi
James Laudenslager
Eugene Laumann
Stuart McDermid
Robert Menzies
Garrett Paine
Thomas Pivirotto
Gary Russell
Carl Thiele

## ABSTRACT

The prospect of the National Aeronautics and Space Administration developing a second generation Ocean Color Scanner has produced the need for coincident *in situ* scientific measurements which examine the primary productivity of the upper ocean on time and space scales that are large compared to the environmental scales of interest. Central to the investigation of the productivity, are questions of the vertical and horizontal variability of the biota, including the relationship between chlorophyll and primary productivity, the productivity of zooplankton, and the dynamic interaction between phytoplankton and zooplankton, and between these populations and the physical environment. To provide these measurements, a towed submersible must be constructed which can accommodate both an underwater LIDAR instrument and a multifrequency sonar. This report includes the requirements for the submersible, and the instrumentation necessary to perform these measurements, and describes the optical and acoustical technology required to develop that instrumentation.

PRECEDING PAGE BLANK NOT FILMED

CONTENTS

## SUMMARY

The upper mixed layer of the ocean is of vital interest in man's interactions with his environment. A significant portion of the world food supply depends on the harvest of the higher trophic levels in the oceans. Our success in that harvest depends on our understanding of the dynamic processes of the food chain, which are governed by the productivity in the upper mixed layer of the ocean. This region is also of interest in attempts to describe the dynamic processes of climate-related phenomena because the global budget of carbon-dioxide may be regulated to a significant extent by physical processes which occur near the sea surface. Because this region exhibits considerable physical and biological activity, the biological species exhibit patchiness at all scales, and for all trophic levels. Thus, to examine the food chain in adequate detail, dynamic models must be formulated based on measurements of the distribution of the various trophic levels, and of the physical structures which influence them, over time and space scales that are large compared to the environmental scales of the region of interest, and that reflect the distribution of these trophic levels throughout the world's oceans. The difficulties in formulating these models, particularly in frontal regions or in dynamic features such as warm core rings, result in part from our lack of understanding of the dynamics of the three-dimensional distributions of the phytoplankton and zooplankton communities.

To formulate these models, the NASA Satellite Ocean Color Science Working Group has recommended that data from the next generation Ocean Color Scanner be coupled with data measured remotely from aircraft and from multiple *in situ* platforms to increase our understanding of the productivity, and of the net uptake of carbon by the marine biosphere. The satellite instruments presently available can provide synoptic measurements of ocean surface temperature using both microwave and infrared radiometry, and measurements of surface wind-driven waves using radar scatterometry. Images of the horizontal distribution of chlorophyll, and of the diffuse attenuation coefficient can be provided by ocean color scanners such as the CZCS. The use of aircraft in these experiments permits the monitoring of surface features which must be covered repeatedly during a period of a few hours. These instruments provide measurements of the surface color, the near-surface vertical distributions of chlorophyll, the near-surface temperature and salinity profiles, and the sea-surface temperature.

To complement these remote observations, shipboard measurements of the physical parameters of the water column can provide the vertical structure of temperature and salinity, the distributions of suspended particulate matter, phytoplankton and zooplankton species distributions, and water samples for chemical analysis. These measurements are essential for the *in situ* calibration and verification of remotely measuring instruments, and to provide *in situ* coincident scientific measurements.

For the monitoring of regional features that exhibit significant long-term variability, the use of moored arrays of sensors can provide long time-series measurements of the biological and physical parameters that define the dynamics of the region, including vertical profiles of temperature and current, local measurement of suspended particulate matter, nutrients, and chlorophyll. To provide measurements of the along-track two-dimensional (vertical) physical and biological properties of the water column for correlations with two-dimensional (horizontal) surface images of ocean color provided by an ocean color scanner, a towed submersible must be used that has the capability of acquiring measurements in the region between the surface and a suitable depth below the seasonal thermocline.

These global observational techniques rely on chlorophyll as an indicator of biomass, and thus provide a partial understanding of the dynamics of the food chain through observations of the intermediate trophic levels. The basic assumption is that remote sensing from above the sea, combined with remote sensing from within the ocean, will be truly synergistic, providing three-dimensional insight to the relations between physics and biology.

## SCIENTIFIC RATIONALE

To achieve an understanding of these processes, it is important to understand the relationship between phytoplankton productivity and the vertical and horizontal variability of the ocean, including the relationship between chlorophyll abundance as a measure of biomass and phytoplankton productivity, the productivity of zooplankton in the upper mixed layer, the dynamic interactions between phytoplankton and zooplankton, and the roles that these trophic levels play in the dynamics of the food chain. The specific questions that can be addressed by this research are the relationship between remotely sensed biomass and primary production, and the relationship between the three-dimensional distribution of chlorophyll and the surface images observed by the CZCS. This latter question includes the description of the coupling of deep populations of phytoplankton and zooplankton with the near-surface populations, the role of physical dynamics in that coupling, and the relationship between specific phytoplankton color groups, zooplankton species, and the physical regime.

The phytoplankton species are distributed vertically through the water column with stratification occurring among their populations. The vertical distributions frequently exhibit a maximum abundance, the deep chlorophyll maximum, located at three to four optical attenuation depths below the surface. Present theories suggest that biological effects are most pronounced at horizontal scales of hundreds of meters to kilometers, with temporal scales of hours to days. Regional features such as the dynamics of ocean currents, or of frontal systems, are often observable using the biology as an indicator. These features can occur on horizontal scales of hundreds of kilometers, and times of weeks to months.

Phytoplankton biomass, while an important factor, does not control the productivity of the ecosystem alone. Zooplankton play a critical role in the transfer of primary production up the food chain and in establishing equilibria in the spatial and temporal distributions of phytoplankton species. The diurnal migration of zooplankton, and the patchiness which is observed at all scales, results in a dynamic pattern of zooplankton grazing that depends strongly on species behavior, and on the distribution and dynamics of the phytoplankton community. These patterns depend on the horizontal variability introduced by the turbulent mixing of nutrients into the euphotic zone through the thermocline, and on the dynamics of the frontal structures along which changes in the biological communities are observed to occur. The variability of the phytoplankton-zooplankton interactions is of key scientific interest in describing the effects of biology on the spatial and temporal variability of ocean color. This variability has in turn placed considerable doubt on theories or concepts based on average values over large spatial or temporal scales.

To understand these dynamic processes, the strong correlation between the physical parameters and the biological distributions must be understood. The measurement of temperature and salinity are essential in understanding the dynamics of these distributions, and in interpreting remote observations. The optical properties of the ocean are also important in an investigation which seeks to link the variation of physical properties with the distribution of biological communities in the surface mixed layer. The absorption and scattering of the incident solar radiation governs the amount of energy available for photosynthesis in phytoplankton, and thus influences the lowest trophic levels. To study this phenomenon, it is necessary to obtain an accurate measure of the spectral irradiance in the water, and to measure those parameters which affect the transmission of radiant energy, including the diffuse attenuation coefficient.

To investigate the horizontal and vertical variability of these populations at all scales, multiplatform measurement strategies must be used. Present studies of ocean color using satellite instrumentation give a synoptic view of the biological and physical features with a horizontal resolution of kilometers. To complement the synoptic measurements, the shorter time scales available through the use of aircraft and ships are essential for the measurement of the dynamics of patches because the times required for their establishment and clearing are often below the Nyquist period of satellite observations. However, remote techniques cannot, by themselves, be used to explain the processes that determine these features because they have no probability of viewing to depths of more than two diffuse attenuation lengths because of the absorption in the water column. Estimates based on available data indicate that substantially less than half of the chlorophyll in the water column is seen by the CZCS at two optical depths based on the integrated spectrum, accounting for approximately half of the total phytoplankton productivity of the water column. Remote *in situ* measurements from a towed submersible LIDAR and acoustics system can be used to examine both the vertical and horizontal variability of physical and biological variables on smaller scales that complement data obtained otherwise by ships and moorings. These measurements will provide insight to the physical and biological phenomena

which underlie and help determine the surface structure observed by aircraft- and satellite-borne remote instrumentation, and permit the correlation of the biological populations with the physical environment.

## TECHNOLOGY REQUIREMENTS

To provide vertical profiles of phytoplankton and zooplankton distributions through the water column, from below the seasonal thermocline to the surface, a towed submersible must be constructed which can accommodate both an underwater LIDAR instrument and a multifrequency sonar. This submersible should include instrumentation to remotely measure the salinity and temperature distributions to an accuracy that is sufficient to resolve biologically important fronts. An upward-looking echosounder or pressure gauge should be included for measuring the vehicle depth, and a system should be constructed that is capable of real-time display and analysis of the data.

To maximize the return of scientific data, the spatial resolution and spatial coverage should be comparable for both the acoustical instrumentation and for the LIDAR. The minimum penetration depth should be 2 to 3 diffuse attenuation depths above and below the vehicle. Range-gating is required to achieve a vertical resolution of 1 m. The horizontal spacing between samples should be approximately 10 m because of the assumption that horizontal diffusion creates isotropy on scales that are small compared to the length scale for patchiness. Either simultaneous measurements of the phytoplankton and zooplankton populations are required in the same volume, or the measurement of statistically similar volumes must be made for the intercomparison of these populations.

## OPTICAL TECHNOLOGY

The accomplishment of these goals will require the use of sophisticated laser and optical spectral analysis technology. The light source should be a pulsed blue-green laser with a pulse length of 5 ns and a pulse repetition rate of 10 to 100 Hz. The return signal should be spectrally resolved using range-gated multi-channel analyzer receivers. The high output power and high efficiency of excimer lasers makes them attractive for oceanographic applications. The XeCl laser system has an output wavelength of 308 nm. This laser radiation can be shifted to the blue-green (459 nm) by near-resonant stimulated Raman scattering.

Remote observations of the physical structure have used the water-stretch Raman measurements to infer the optical properties of the water column, and the temperature. Raman scattering occurs as an interaction between the incident light field and the thermally excited molecular vibrations of water. The integrated intensity of the Raman band can be used to measure the diffuse attenuation coefficient as a function of depth by accounting for the attenuation at the transmitted and Raman shifted wavelength. The temperature can be measured by examining the depolarization of the Raman-shifted light.

To complement these measurements, Brillouin scattering techniques have been used for the measurement of the local sound speed in water. Brillouin scattering occurs as an interaction beteeen the incident light field and ultrasonic waves produced as a result of turbulent processes. The resulting photon-phonon scattering produces a symmetric pair of lines, centered on the incident laser line, and separated from it by a wavelength that is proportional to the sound speed in the water. In regions of strong salinity gradient, the use of a combined Raman-Brillouin system may be required to estimate the temperature and salinity.

The spectral reflectance from pigmented phytoplankton is a measure both of the particle size through Mie scattering and of the absorption by the pigments. The absorption and the fluorescence efficiency of chlorophyll a, and of other pigments, reveals the state of health of the phytoplankton and the distribution of chlorophyll-related biomass. By excitation and detection using multiple wavelengths between 440 nm and 510 nm, to take advantage of the minimum in the absorption spectrum and of the optimum excitation wavelengths for chlorophyll fluorescence, spectral reflectance, and species identification, the taxonomic composition of the phytoplankton can be determined in a manner similar to the measurement of chlorophyll by the CZCS. The receiver should examine the fluorescence bands of phycoerythrin at 585 nm, and chlorophyll at 685 nm, for near-field measurements of the chlorophyll-related biomass.

## ACOUSTICAL TECHNOLOGY

The measurement of zooplankton populations can be made by in situ remote measurements of acoustical backscattering from layers of high zooplankton concentrations using an acoustic analyzer based on a chirp sonar. This approach will provide a simultaneous vertical along-track profile which can be used to describe the distribution of zooplankton populations and the interrelationship between zooplankton and the physical and biological environment.

Two properties of acoustical systems are important in determining their performance, the maximum range and the range acuity. The maximum range over which a target can be detected is determined by the signal-to-noise ratio of the instrument, and is frequency dependent because of differential absorption in the water column. The signal-to-noise ratio for detection of acoustical backscattered energy depends on the transmitted energy, the receiver sensitivity, and the logarithm of the acoustic scattering cross-section of the organisms under study. The use of a linear frequency-modulated sonar, based on the principles of chirp radar, will substantially enhance the transmitted energy over that available using a single-frequency ping system while maintaining the desired range resolution. The backscattering cross section can be evaluated theoretically by using a scattering model. Existing scattering models are a good approximation for euphausiids and sergestid shrimp, but not for copepods, which exhibit a distinctive orientational dependence of the scattering cross section.

## RESEARCH REQUIRED

Several areas of instrument technology development and research are required to design a towed submersible instrument. Quantitative data on the signal and noise levels to be expected for Brillouin and Raman scattering are needed. Quantitative data on the signal levels to be expected for the spectral reflectance in selected bands, and the optimum bands to be used for the measurement of chlorophyll concentrations, are needed. Quantitative data on the signal levels to be expected for the 685 nm chlorophyll a fluorescence band are needed for varying water conditions, and investigations of the underwater propagation of laser light are needed. A theoretical analysis, substantiated by laboratory measurements, is needed to determine the spectral irradiance (watts/cm$^2$ per wavenumber) on the entrance aperture of a submersible instrument for the measurement of Raman, Brillouin, turbidity, fluorescence, and backscatter signals. The algorithms required to analyze these data, and to produce information on the structure of the physical and biological features in the water are also needed.

Quantitative data are also required which permit the comparison of a chirp sonar directly to a ping sonar having the same range acuity, frequency, and pulse intensity. This comparison will permit the assessment of these two techniques and the evaluation of the anticipated signal-to-noise ratio enhancement from the chirp sonar. Quantitative data are required to define the detailed nature of the scattering of acoustic signals from zooplankton populations, including the dependence on size distributions and species types. For this assessment, measurements are required of individual target strengths, and additional modeling is required to extend the measurements to the backscattered signal obtained from collections of individuals of various species. Effects of non-spherical scatters and scattering from multiple targets should be included in these analyses.

# SECTION I

## INTRODUCTION

Production of a significant portion of the world food supply depends on the harvest of the higher trophic levels in the oceans. The upper ocean is the primary region of interest in attempts to describe the dynamic processes of the food chain, which in part determine our success in that harvest. These processes are governed by the productivity in the upper ocean, extending tens of meters from the ocean surface to below the seasonal thermocline. This region is also of interest in attempts to describe the dynamic processes of climate-related phenomena because the global budget of carbon-dioxide may be regulated to a significant extent by physical processes which occur near the sea surface. Because this region exhibits considerable physical and biological activity, the biological species exhibit patchiness at all scales and for all trophic levels (cf. Steele, 1978, Haury, et al., 1978). Thus, to examine the food chain in adequate detail, dynamic models must be formulated that reflect the distribution of trophic levels throughout the world's oceans. These models must be based on measurements of the distribution of trophic levels over time and space scales that are large compared to the environmental scales of the region of interest. The difficulties in formulating these models, particularly in frontal regions, or in dynamic features such as warm core rings, result in part from our lack of understanding of the dynamics of the three-dimensional distributions of the phytoplankton and zooplankton communities.

Remote observations of the ocean are presently underway both from satellites and from aircraft. Because the ocean is relatively opaque to electromagnetic radiation, the depths attainable by remote observational techniques depend on the wavelength used. Microwave measurements of the sea-surface temperature average over one wavelength in depth (cf. NASA, 1980). In contrast, the Coastal Zone Color Scanner (CZCS), (cf. NASA, 1980, Carder, 1981, Hovis, et al., 1980) provides two-dimensional images of the upper ocean, on a global scale, which are formed by a weighted return from approximately the first optical attenuation depth in the water column. An optical attenuation depth is defined as the depth at which light is attenuated to 1/e of its surface value, and thus changes with wavelength.

To complement these measurements, present aircraft-borne oceanic LIDAR (Light Detection and Ranging) can measure the temperature distribution in the first optical attenuation depth to an accuracy comparable to that achieved for sea-surface temperature from a satellite (cf. Leonard, et al., 1979, Leonard, 1980, Carder, 1981). The measurement of chlorophyll abundance, using the fluorescence excited by an airborne oceanic LIDAR, has a present accuracy (~ 30%) in the first optical attenuation depth that is comparable to the accuracy attainable by <u>in situ</u> fluorometers (cf. Carder, 1981, Bristow, 1978, Bristow, et al., 1979, Smith, et al., 1982).

Preliminary conclusions from the NASA Satellite Ocean Color Science Working Group (J. Walsh, personal communication) are that improved models using data from the next generation CZCS and multiple *in situ* platforms, including a towed LIDAR and acoustics sensor, are necessary to increase our understanding of the productivity and of the net uptake of carbon by the marine biosphere. As a step toward the realization of these goals, Smith, et al., 1982, used the CZCS to examine the primary productivity in the Southern California Bight and noted a marked decrease in the productivity over a period of less than two weeks during March, 1979. These determinations depended upon both the CZCS and on a relatively accurate model of the productivity per unit chlorophyll for the region under spring topographic upwelling conditions, during which plankton nutrient availability covaries closely with negative temperature anomalies. In this region, sea-surface temperature, chlorophyll, and daylength account for nearly 70% of the variability in primary productivity. For different seasons or other locations, more complex models may be needed and a means of rapidly measuring phytoplankton and zooplankton distributions may be required.

These global observational techniques rely on chlorophyll as an indicator of biomass, and thus provide a partial understanding of the dynamics of the food chain through observations of the intermediate trophic levels. One difficulty in interpreting these measurements arises from the fact that the thermocline and the chlorophyll maximum often occur at depths in excess of three to four optical attenuation lengths, depending upon season, weather, and location. Thus, to provide physical and biological interpretation of the information contained in the CZCS images, it is important to understand the dynamic three-dimensional ocean processes that create them, including, for example, the effects of upwelling on phytoplankton productivity, the effects of internal waves on the variability of the chlorophyll maximum, and the complex interaction between phytoplankton and zooplankton. Such measurements can only be made by *in situ* instruments which have the capability of examining the two-dimensional physical and biological structure of the euphotic zone of the ocean.

This study explores the biological and physical oceanographic investigations needed to place the remote observations in context. The measurements, and the technology required to perform them, will be defined in the light of currently available technology and of existing measurement programs, and with a view toward the technological developments required for future investigations. The emphasis is on optical and acoustical techniques that will permit remote observations from underwater platforms, and on the requirements for the platforms themselves.

The basic assumption is that remote sensing from *above* the sea, combined with remote sensing from *within* the ocean, will be truly synergistic, providing three-dimensional insight to the relations between physics and biology.

## SECTION II

## SCIENTIFIC RATIONALE

The principal scientific goal of this program is to understand the dynamics of the food chain in the upper mixed layer of the ocean. To achieve this goal, it is important to understand the relationship between phytoplankton productivity and the vertical and horizontal variability of the ocean on spatial and temporal scales which are large compared to the environmental scales of the region of interest. Included in the study of phytoplankton productivity are investigations of the relationship between chlorophyll abundances as a measure of biomass and phytoplankton productivity, the productivity of zooplankton in the upper mixed layer, the dynamic interactions between phytoplankton and zooplankton, and the roles that these trophic levels play in the dynamics of the food chain.

The specific questions that can be addressed by this program are the relationship between remotely sensed biomass and primary production, and the relationship between the three-dimensional distribution of chlorophyll and the surface images observed by the CZCS. This latter question includes the description of the coupling of deep populations of phytoplankton and zooplankton with the near-surface populations, the role of physical dynamics in that coupling, and the relationship between specific phytoplankton color groups, zooplankton species, and the physical regime.

Figure 1 indicates the spatial and temporal regimes for each of the taxonomic groupings, and a measure of the overlap between trophic levels (cf. Steele, 1978, Haury, et al., 1978). Also included in this figure are the regimes of spatial and temporal coverage accessible by the various measurement systems (cf. Esaias, 1980). To investigate the variability of these populations at all scales, multiplatform measurement strategies must be used. Remote *in situ* measurements using LIDAR and acoustics techniques, for example, can be used to examine both the vertical and horizontal variability of physical and biological variables on scales that complement data obtained otherwise by ships and moorings, and the more synoptic data obtained remotely by aircraft and by satellites. The short time scales available through the use of aircraft and ships are essential for the measurement of the dynamics of patches because the times required for their establishment and clearing are often below the Nyquist period of satellite observations, which is determined by the repeat period and thus subject to weather constraints.

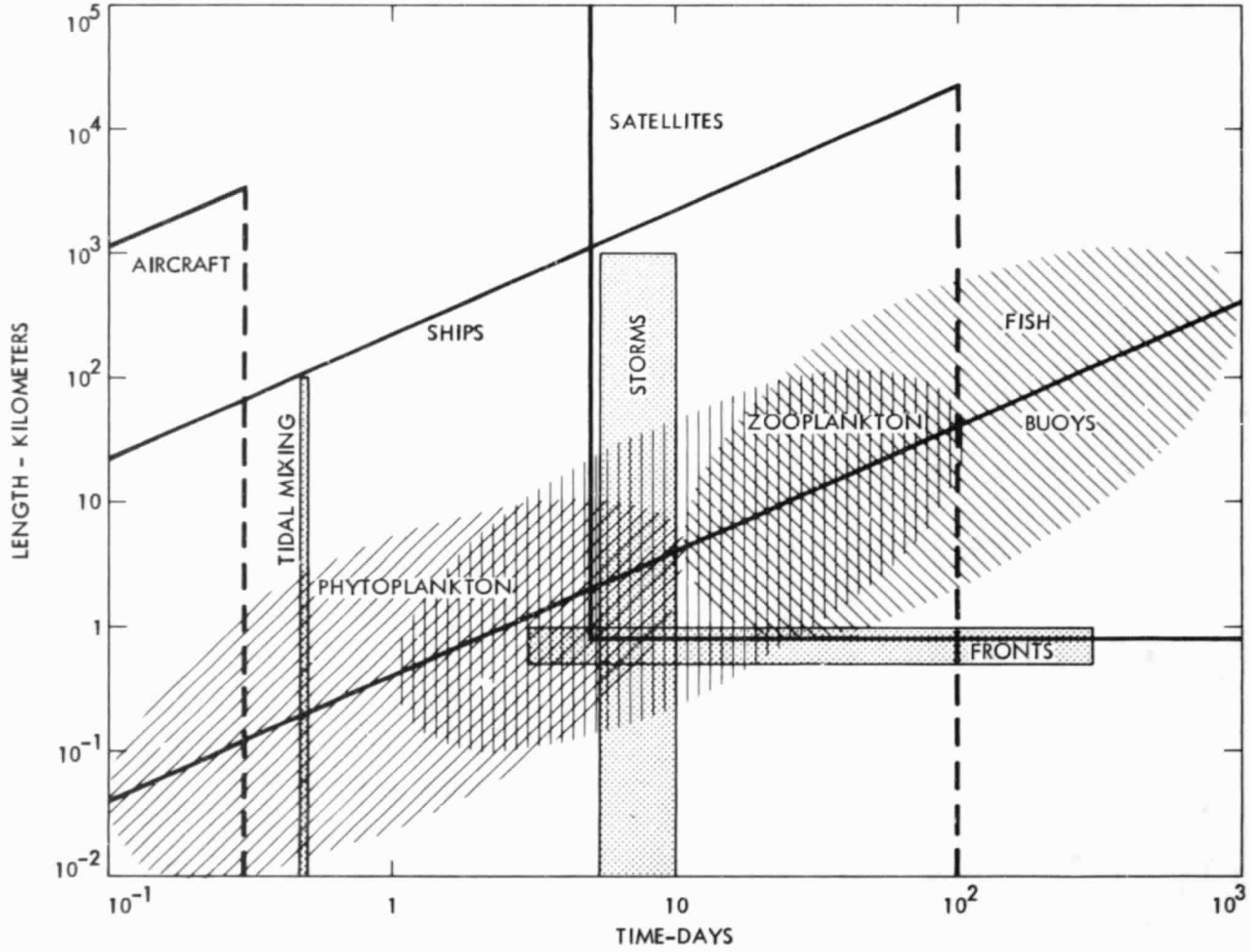


Figure 1. Space-Time Domains for Oceanic Phenomena
(Adapted from Steele, 1978 and Esaias, 1980)

ORIGINAL PAGE IS
OF POOR QUALITY

## A. PHYTOPLANKTON

The phytoplankton species of interest range in size from 3 μm to 200 μm equivalent diameter (cf. Eppley, et al., 1977, Pugh, 1978). These species are distributed vertically through the water column, with stratification occurring among their populations, on a vertical scale of meters or less. The vertical distributions of phytoplankton frequently exhibit a maximum abundance, the deep chlorophyll maximum, located at three to four optical attenuation depths below the surface, often within the seasonal thermocline. The smallest scales for phytoplankton patchiness range from centimeters, created by the interleaving of temperature and salinity structures in the thermocline, producing turbulent vertical microstructure on a time scale of seconds, to meters created by horizontal variability in physical structure on a time scale of minutes. Such vertical fine structure is of ecological interest but lies below the sensitivity of the instrumentation considered here.

The horizontal variability of these populations occurs at all scales. At scales less than 100 m, where species differences may be important, the cells respond as passive tracers for the physical motions because insufficient time exists for a biological response to the dynamics of the system. Present theories suggest that biological effects are most pronounced at horizontal scales of hundreds of meters to kilometers with temporal scales of hours to days. Regional features such as the dynamics of ocean currents, or of frontal systems, are observable using the biology as an indicator (cf. Esaias, 1980). These features can occur on horizontal scales of hundreds of kilometers and times of weeks to months, as illustrated in Figure 1 (cf. Steele, 1978, Haury, et al., 1978). Advances in our understanding depend upon integrating information on the growth of the plants, grazing by herbivores, and local patterns of circulation, advection, and mixing. The measurement of the number density and biological activity of individual species in a region is of interest, together with the distribution of sizes.

The characteristic signatures of individual plant species (cf. Yentsch and Yentsch, 1979) may be found in the spectral reflectance, which measures the absorption of light by the pigments, and in the fluorescence from pigments, including the bands caused by gelbstoffe at 570 nm and from chlorophyll at 685 nm, as shown in Figure 2. The physiological status and taxonomic composition of these populations can be determined in part from the ratios of phycoerythrin to chlorophyll, of carotenoids to chlorophyll, and of the Mie scattering return to the amplitude of one or more of the fluorescence emissions. Phytoplankton species diversity among algal color groups has been measured (cf. Jarrett, et al., 1979., Esaias, 1980) using multiple excitation wavelengths to produce the fluorescence return, thus determining the fluorescence efficiency of the individual groups. These multiple wavelength techniques can be used to detect changes in the species composition, both vertically and horizontally through the water column, and to give a measure of the chlorophyll-related biomass of the system. However, the effects of light history, temperature, and the distribution of nutrients on the fluorescence yield, remain as complications in the remote measurement of species diversity.

ORIGINAL PAGE IS
OF POOR QUALITY

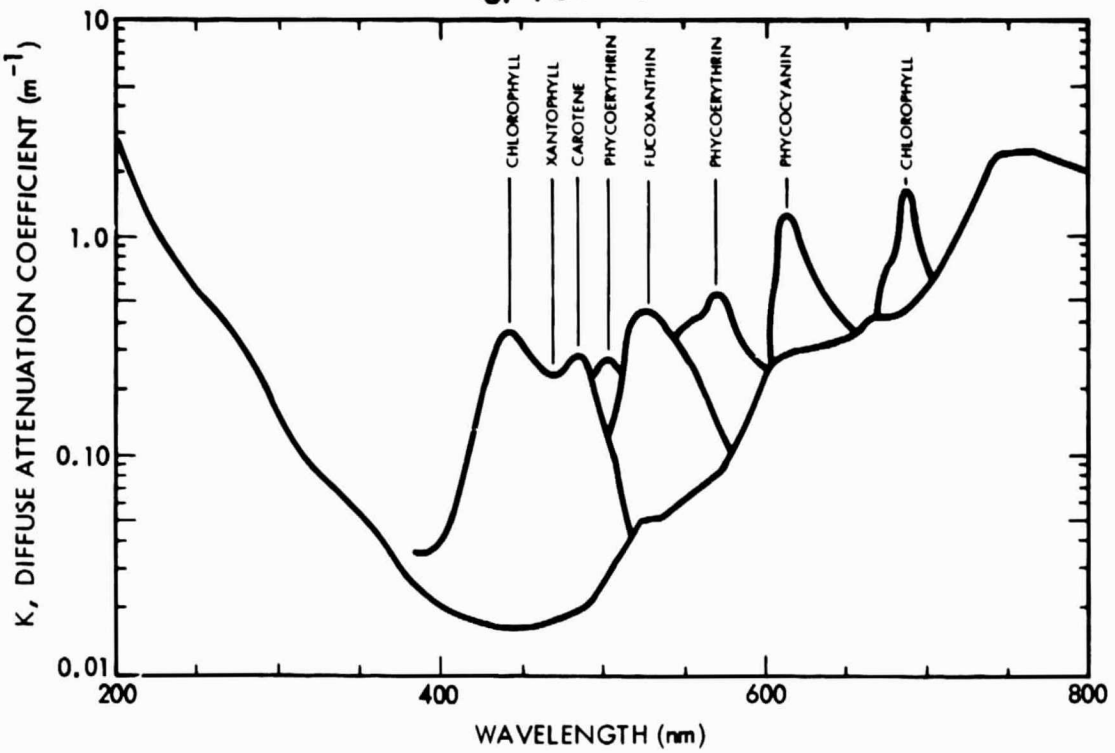


Figure 2. The diffuse attenuation coefficient as a function of wavelength. An illustration of the excitation and emission spectra of pigments. Excitation and emission spectra from Yentsch and Yentsch, 1979.

To determine the productivity of the phytoplankton, their vertical distribution through the euphotic zone, from below the chlorophyll maximum to the surface, must be known. This structure must then be related to the distribution of zooplankton species, and to the distribution of the physical and nutrient properties of the water column. The growth dynamics and rate processes of both plants and animals must be studied in sufficient detail to understand their dependence on the dynamics of the mixed layer, including the turbulent structure near the chlorophyll maximum. To understand these dynamic processes, the energetics of the exchange of nutrients, carbon, and oxygen between the water and the organisms must also be studied.

Present studies of ocean color using the CZCS are limited by the portion of the water column available for measurement. Estimates based on available data, illustrated by Figure 3 (Cullen and Eppley, 1981, Smith, 1981), indicate that substantially less than half of the chlorophyll in the water column is seen by the CZCS at two optical depths based on the integrated spectrum, accounting for approximately half of the total phytoplankton productivity of the water column. Because the chlorophyll maximum occurs at three to four optical attenuation depths in the 480 nm to 510 nm band, where minimum absorption occurs, or four to five optical

attenuation depths based on the visible spectral band, the chlorophyll maximum is not accessible to present remote sensing techniques (cf. Carder, 1981, Bristow, et al., 1980, Smith, 1981). The CZCS image shown in Figure 4 (cf. Smith and Baker, 1982) gives a synoptic view of changes in ocean color on a horizontal scale of kilometers, but cannot, by itself, be used to explain the processes that determine these features. These dynamic regions require detailed spatial and temporal observations for complete understanding. The instantaneous distribution of ocean color has been translated to the distribution of chlorophyll through algorithms developed by Smith and Baker, 1982 and by Gordon, et al., 1980. Observation using aircraft during daylight hours (Figure 1) can provide the detailed distributions of chlorophyll and temperature (Leonard, 1980, Bristow, et al., 1980) to depths of one or two diffuse attenuation lengths. However, we have no probability of viewing these features to depths of more than two diffuse attenuation lengths using aircraft- and satellite-borne remote measurement techniques (cf. Esaias, 1980) because of the absorption in the water column.

## B. ZOOPLANKTON

Phytoplankton biomass, while an important factor, does not control the productivity of the ecosystem alone. Zooplankton play a critical role in the transfer of primary production up the food chain, and in establishing equilibria in the spatial and temporal distributions of phytoplankton species. The zooplankton species of interest range in size from 100 μm to 10 cm (cf. Holliday and Pieper, 1980, Herman and Mitchell, 1981), and include both herbivores and carnivores. The vertical distributions of these species are highly stratified and can change as a function of physiological state, age, and time of day.

The characteristic signatures of the individual zooplankton species are not well known. The bioluminescence characteristics of individual species, to the extent that such signatures exist, may give an effective means of classifying individual species or groups, providing sufficiently distinct and consistent spectral signatures can be obtained by laboratory and field analysis. For these measurements, the light history of bioluminescence may be measured using photometers having a suitable spectral and temporal resolution.

The acoustic signatures of zooplankton size classes can be determined (Holliday and Piper, 1980) using both the scattering cross-section or target strength of individual species, and by observing resonances with swim bladders and other species-specific structures. The target strength is a function of the differential acoustic impedance between the individual and the background, depending both on differential compressibility and on differential density, and is a function of the orientation of individuals having an aspect ratio differing substantially from unity. These effects may be determined by obtaining the spectrum from individuals using appropriate multiple-frequency techniques.

ORIGINAL PAGE IS
OF POOR QUALITY

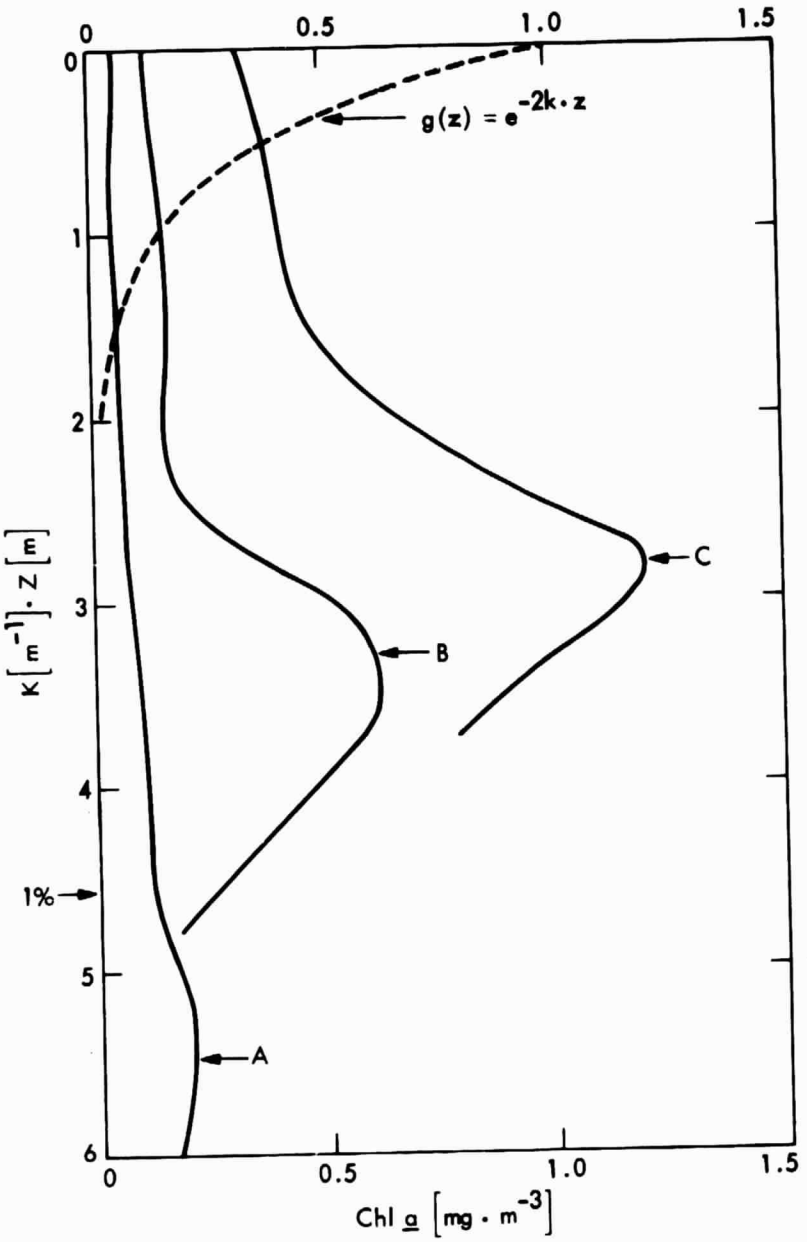


Figure 3. The distribution of chlorophyll as a function of optical depth. (A) North Pacific Gyre (28°N, 155°W) from Beers, et al., 1975; (B) SCBS 15, Sta. 205; (C) SCBS 7, Sta. 102 from Cullen and Eppley, 1981, Adapted by Smith, 1981.

ORIGINAL PAGE
BLACK AND WHITE PHOTOGRAPH

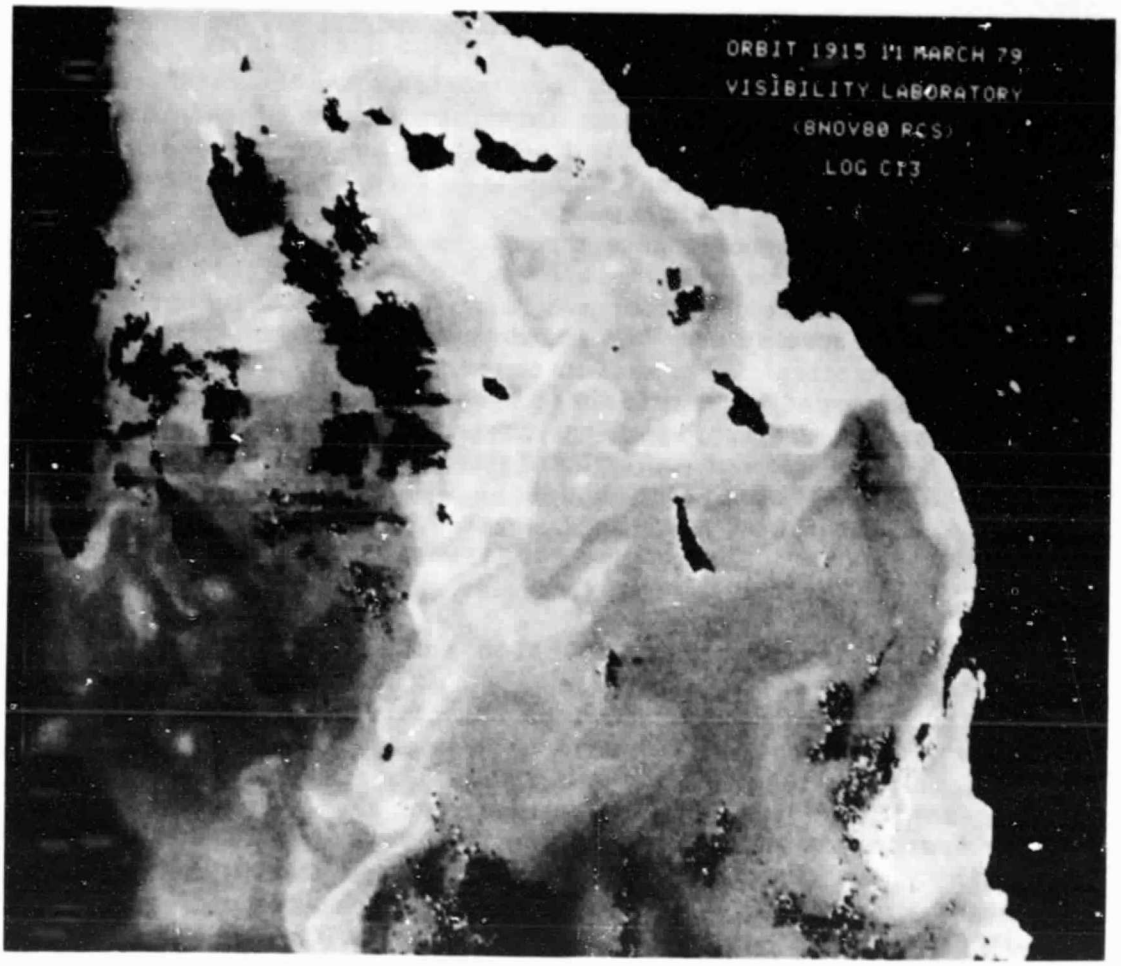


Figure 4. The Southern California Bight Viewed from the Nimbus-7 Coastal Zone Color Scanner. Photograph courtesy of R. Smith (cf. Smith and Baker, 1982).

## C. PHYTOPLANKTON - ZOOPLANKTON INTERACTIONS

The dynamics and near-surface variability of phytoplankton-zooplankton interactions are of key scientific interest in describing the effects of biology on the spatial and temporal variability of ocean color. This variability has in turn placed considerable doubt on theories or concepts based on average values over large spatial or temporal scales.

The diurnal migration of zooplankton, and the patchiness which is observed at all scales, results in a dynamic pattern of zooplankton grazing that depends strongly on species behavior, and on the distribution and dynamics of the phytoplankton community. These patterns depend, in part, on the horizontal variability introduced by the turbulent mixing of nutrients into the euphotic zone through the thermocline. The transport of nutrients may also be responsible for the vertical offset between the phytoplankton and zooplankton maxima. To study these phenomena, the distribution of species near the chlorophyll maximum must be measured, and sufficient statistical information obtained, to adequately describe the patchiness observed within trophic levels, and its correlation with the observed physical properties of the layer. These measurements will often depend on the dynamics of the frontal structures along which large changes in the biological communities are observed to occur. This dynamic behavior includes the turnover of the water mass above the thermocline, and is critically dependent on the relationship between the spatial and temporal scales for the dynamic processes and for the biology.

On a larger scale, advection and mixing may create vertical displacements in the thermocline, and in the deep chlorophyll maximum. These effects can be found in regions of coastal upwelling, where vertical velocities of the order of 0.1 mm/s produce a substantial flux of nutrients upward into the euphotic zone, and in the passage of internal waves. The surface manifestations of these phenomena are changes in the observed surface temperature (cf. Gower, et al., 1980, Vukovich and Crissman, 1980) and salinity, and substantial changes in surface layer chlorophyll, caused by changes in ambient light, by nutrient flux changes, and by an increase in chlorophyll density. These effects can be observed by remote techniques (Esaias, 1980, Gordon, et al., 1980). Other examples of combined vertical and horizontal processes are the advective motions generated by eddy diffusion, by Langmuir circulation, by warm-core rings, and by regional gyres.

The distribution of higher trophic levels in the food chain depends on the grazing dynamics of these species, especially on the schooling, aggregation, and mobility of the larger species. These distributions depend partially on the detailed distributions of the lower trophic levels but especially on the cycle or ambit of migration of the larger species. This range depends also on the temperature and salinity of the water mass at larger scales, but the biological factors may be the most restrictive.

## D. OCEANIC VARIABILITY

To understand these dynamic processes, the strong correlation between the physical parameters and the biological distributions must be understood. For example, the thermal and density structures that exist near the thermocline influence the biological productivity and serve to concentrate the biological species in narrow bands that seem to be locked to that structure. Fluctuations of the chlorophyll maximum are often associated with such structures. The measurements of temperature and salinity are essential in understanding the dynamics of these distributions, and in interpreting remote observations.

Existing temperature measuring techniques using expendable Bathythermograph (XBT) or thermistor chains have limitations in defining the vertical distribution through the water column along the track of a ship. To produce a vertical resolution of 1 m in remote measurements made 20 m or more from a source, range-gated optical techniques must be found to produce these measurements to the accuracies required. The use of the Raman return presently yields data with a resolution in excess of one degree (cf. Leonard, et al., 1979, Leonard, 1980). Although this technique can be improved, it is unlikely that the resolution can be improved substantially below 0.5°C. Such resolution will be required to make this technique useful for the examination of the thermal structure. As a complementary technique, Brillouin scattering, the scattering of light from acoustic waves in water, measures the speed of sound in the water, and gives a frequency shift dependent on both temperature and salinity (Hirschberg, et al., 1977). Although early measurements have not given accurate results, calculations support temperature resolution substantially better than one degree. The salinity must be measured separately, perhaps by the use of a combination with Raman measurements, to produce this accuracy.

These or other techniques can be used to measure the vertical distribution of temperature and density in the water column. By comparing these measurements to an absolute measure of both the temperature and salinity at one depth, the vertical structure of temperature can be deduced.

The optical properties of the ocean are an important part of an investigation which seeks to link the variation of physical properties with the distribution of biological communities in the surface mixed layer. The absorption and scattering of the incident solar radiation (cf. Zaneveld and Spinrad, 1979, Gordon, 1980, Simpson and Dickey, 1981) governs the amount of energy available for photosynthesis in phytoplankton, and thus influences the lowest trophic levels. To study this phenomenon, it is necessary to obtain an accurate measure of the spectral irradiance in the water and to measure those parameters which affect the transmission of radiant energy, including the diffuse attenuation coefficient. Thus, the absorption spectra shown in Figure 2 (Smith and Baker, 1981), the surface-layer scattering, and the scattering and polarization effects of suspended particulate matter in the water column are important physical phenomena to study.

## E. RATIONALE FOR REMOTE IN SITU MEASUREMENTS

The dynamic processes shown in Figure 4 cannot be properly interpreted without measuring the vertical structure of the physical and biological properties of the water column in the region between the seasonal thermocline and the surface. This vertical structure can be obtained by using a towed submersible containing a range-gated LIDAR system designed for underwater applications as illustrated in Figure 5. This system can measure the chlorophyll-related biomass by the use of multiple wavelength optical excitations to examine the distribution of phytoplankton abundances by measuring the spectral reflectance and emission spectra from chlorophyll and other pigments. The Rayleigh scattering return can be used to monitor the particulate number density and Brillouin and Raman scattering can be used to measure the temperature and salinity distributions. These measurements provide insight to the physical and biological phenomena which underlie, and help determine, the surface structure observed by aircraft- and satellite-borne remote instrumentation. Simultaneous measurements of the distribution of zooplankton abundances can be made by an in situ acoustic analyzer based on a chirp sonar. Two-dimensional vertical spatial resolution of 1 m can be obtained by range-gating the measurements 2 to 3 diffuse attenuation depths above and below the vehicle. Transects made either at constant depth, or at lines of constant $\sigma_T$ can then provide both verification of the remotely sensed measurements and coincident measurement of independent variables.

ORIGINAL PAGE IS
OF POOR QUALITY

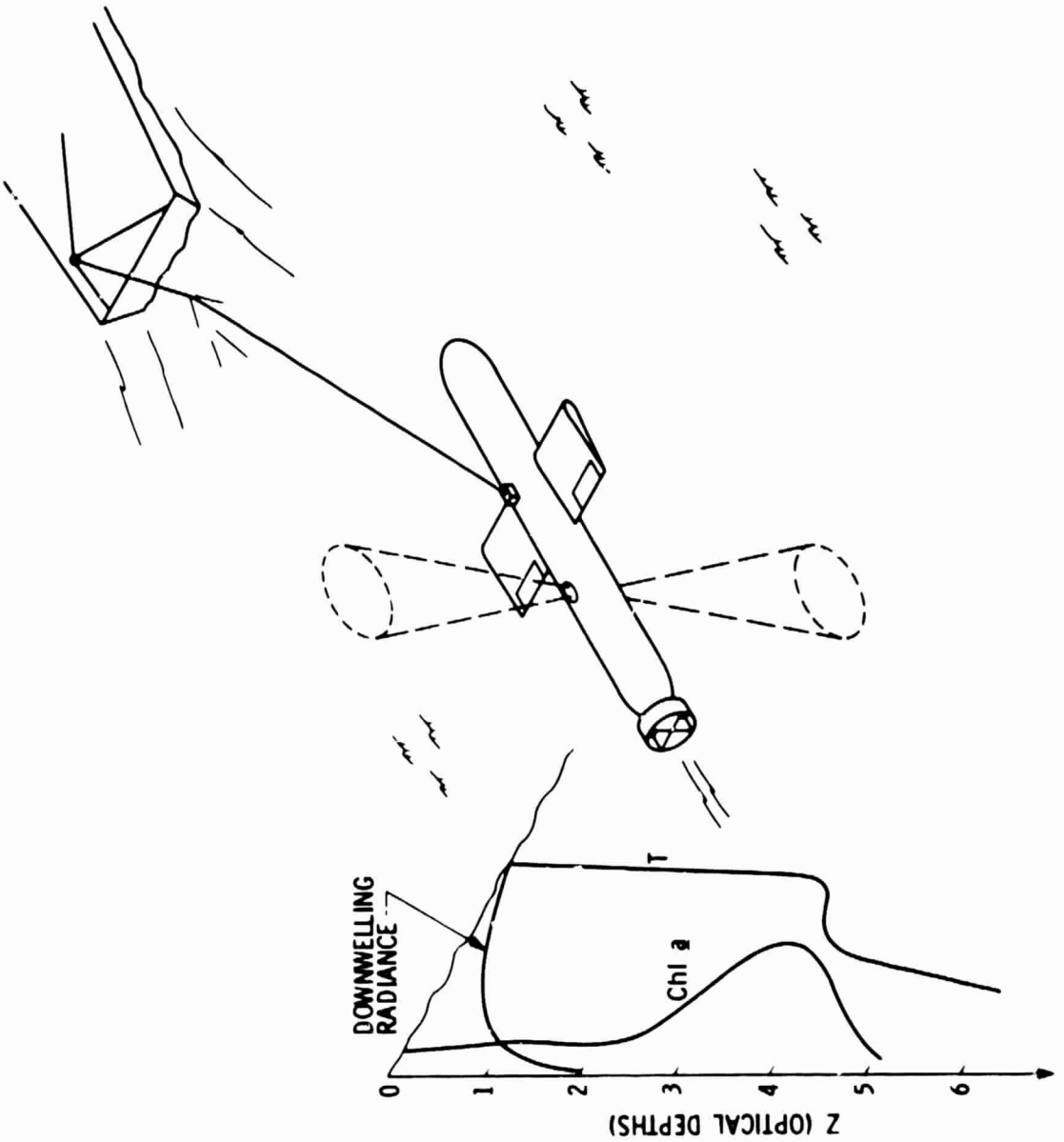


Figure 5. Concept for LIDAR and Acoustics Towed Submersible

PRECEDING PAGE BLANK NOT FILMED

# SECTION III

# EXISTING MEASUREMENT CAPABILITY

Field experiments designed to investigate oceanic productivity are interdisciplinary in nature and involve data from a number of instruments on different platforms. Central to future experiments will be the remote sensing data obtained from satellites as described by Wilson, 1981. These sensors will provide synoptic measurements of ocean surface temperature using both microwave and infrared radiometry (cf. Stewart, 1981), and measurements of surface wind-driven waves using radar scatterometry (cf. O'Brien, 1981). Images of the distribution of chlorophyll and of the diffuse attenuation coefficient (cf. Esaias, 1981) will be provided by ocean color scanners such as the CZCS. These instruments, in concert, maximize the scientific return from surface and *in situ* observations by permitting the regions of interest to be selected in real time from the synoptic data.

The use of aircraft in these experiments permits the monitoring of surface features which must be covered repeatedly during a period of a few hours. Using airborne ocean color scanners and LIDAR instrumentation, measurements of the surface color and of the near-surface vertical distributions of chlorophyll can be obtained from the range-gated return from either single- or multiple-frequency excitations. The near-surface temperature profile can also be measured using either the Raman return or techniques based on Brillouin scattering, and the sea-surface temperature can be monitored using airborne infrared instrumentation. For a description of this instrumentation, see Campbell, et al., 1981. These measurements will permit an intercomparison with the satellite-borne color scanner and thermal sensors.

To complement these observations, shipboard measurements of the physical parameters of the water column can provide the vertical structure of temperature and salinity, the distributions of suspended particulate matter and of phytoplankton and zooplankton species, and water samples for chemical analysis. These measurements are essential for surface truth and for the *in situ* calibration and verification of remotely measuring instruments.

## A. SATELLITE REMOTE MEASUREMENTS

The satellites which have carried instruments relevant to ocean productivity are listed in Table 1 together with the instrumentation on each. These instruments are described (cf. Stewart, 1981) in Table 2, where the accuracy and resolution with which each measurement can be determined are listed together with the spatial area over which the measurement are obtained.

TABLE 1

SATELLITES WITH OCEAN PRODUCTIVITY INSTRUMENTS

| SATELLITE | LAUNCH DATE | INCLINATION (Deg) | ALTITUDE (km) | PERIOD (min) | INSTRUMENTS | OBJECTIVE |
|---|---|---|---|---|---|---|
| Seasat-1 | 6/78 | 108 | 769-799 | 101 | SMMR, SASS | Ocean Geoid Imaging<br>Sea Surface Temperature<br>Wind and Waves |
| Nimbus-7 | 10/78 | 99 | 938-953 | 104 | SMMR, CZCS | Sea Surface Temperature<br>Chlorophyll |
| NOAA-6 | 1979 | 99 | 830 | 102 | AVHRR | Sea Surface Temperature |

AVHRR - Advanced Very High Resolution Radiometer
CZCS - Coastal Zone Color Scanner
SASS - Seasat Scatterometer System
SMMR - Scanning Multifrequency Microwave Radiometer

TABLE 2

SATELLITE INSTRUMENT PERFORMANCE

| INSTRUMENT | SATELLITE | OBSERVABLE | ACCURACY | RESOLUTION | FOOTPRINT |
|---|---|---|---|---|---|
| AVHRR | NOAA-6 | Sea Surface Temperature | ±0.6°C | ±0.2°C | 1.1 km - 4 km pixel |
| CZCS | Nimbus-7 | Chlorophyll | ±30% | ±10% | 800m pixel<br>±40° swath - 1200 km |
| | | Diffuse Attenuation Coefficient | ±15% | ±10% | ±20° tilt from nadir |
| | | Sea Surface Temperature | ±2.0°C | ±0.2°C | |
| SASS | Seasat-1 | Wind Velocity<br>Wind Direction | ±1.6 m/s<br>±16° | | Wind Vector<br>50 km pixel<br>1500 km swath<br>Wind Speed<br>10 km pixel |
| SMMR | Seasat-1<br>Nimbus-7 | Sea Surface Temperature | ±1.0°C | | 150 km pixel |
| | | Wind Speed | ±2.5 m/s<br>no direction | | |

1. Sea-Surface Temperature

The sea-surface temperature has been measured both by infrared and by microwave techniques. Measurements to an accuracy better than $\pm 1^{o}C$ and a resolution of $\pm 0.2^{o}C$ have been made using the Advanced Very High Resolution Radiometer (AVHRR) on NOAA-6. This is an infrared scanning radiometer which monitors the emitted and reflected radiation in four channels including a visible channel at 0.55-0.90 $\mu$m, and three infrared channels at 0.73-1.3 $\mu$m, 10.5-11.5 $\mu$m and 3.55-3.93 $\mu$m. In the absence of clouds, the effects of atmospheric water vapor and aerosols can be removed from the data, and estimates of the sea-surface temperature obtained, using the data from all four channels.

A second infrared measurement of the sea-surface temperature can be obtained using the 11.5 $\mu$m band on the CZCS. The relatively poor resolution in temperature results from the lack of additional infrared channels and from the collecting aperture used. The data are susceptible to interference by clouds and rely on the atmospheric corrections derived from the color algorithms to remove atmospheric effects on the measurement of sea-surface temperature.

Microwave techniques have been employed in the Scanning Multichannel Microwave Radiometer (SMMR) for the measurement of sea-surface temperature. This instrument uses five microwave frequencies with dual polarization on each to obtain $\pm 1^{o}C$ accuracy. These measurements can be made in the presence of clouds without precipitation but are subject to sunglint, to the brightness of adjacent land, and to radio frequency interference effects as well as to the effects of sea-surface roughness.

2. Near-Surface Winds

Microwave and scatterometry techniques have been used to infer the near-surface winds from the local formation of capillary waves. The Seasat-1 Scatterometer System (SASS) measures winds in the range 5 to 24 m/s to an accuracy of $\pm 1.6$ m/s. These measurements encompass $360^{o}$, with a directional accuracy of $\pm 16^{o}$, and a directional ambiguity which is correct 66% of the time. From these measurements, the surface wind stress can be deduced from the off-nadir capillary wave spectrum, and near-surface fluxes can be derived using the other measured physical parameters.

Additional measurements of wind speed are available from the SMMR on Seasat-1 and on Nimbus-7. This instrument provides an accuracy of $\pm 2.5$ m/s in wind velocity but does not give wind direction.

3. Horizontal Distribution of Chlorophyll

The spatial distribution of chlorophyll in the upper portion of the euphotic zone can be determined from the Coastal Zone Color Scanner (CZCS) on Nimbus-7. This instrument (cf. Hovis, et al., 1980) is a passive multispectral radiometer which monitors five channels in the visible portion of the spectrum to evaluate the presence of chlorophyll and other pigments by measuring the upwelling radiance in spectral bands which have

been chosen to provide maximum contrast in the reflectance spectra of chlorophyll-bearing organisms. Algorithms have been developed (cf. Smith and Baker, 1982, Gordon, et al., 1980) to remove the effects of the atmosphere from the signal and to compute the concentrations of chlorophyll and other pigments to an accuracy of ±30% over a range of 0.1 to > 5 μg/l chlorophyll. From these data, the diffuse attenuation coefficient can also be obtained to an accuracy of ±15% over a range 0.01 to 6 $m^{-1}$. These algorithms use the relative intensity of bands in the red portion of the spectrum to assess the rather large atmospheric corrections, thus permitting the extraction of the upwelling radiance from the ocean in each spectral band. The instrument is limited to observations during daylight hours and relatively clear weather, and cannot accurately measure the chlorophyll concentration within 2 to 3 km of the land because of the increased spectral brightness of the land.

## B. AIRCRAFT REMOTE MEASUREMENTS

Aircraft can be used to provide additional instrument capability to augment satellite observations, and to provide temporal coverage with repeat periods of a few minutes to a few hours. The principal aircraft-borne instruments which are presently available are described in the Chesapeake Bay Plume Study Proceedings (cf. Campbell and Thomas, 1981). These include instrumentation for the measurement of chlorophyll concentrations, chlorophyll fluorescence, salinity, and sea-surface temperature. Many of the instruments are large and require a P-3 or other large fixed-wing aircraft for operation. In the future, compact systems may be required for use on aircraft of opportunity rather than on a designated aircraft. The quality of the measurements obtained from these instruments are subject to weather but provide the capability for an increased horizontal resolution and thus a greater spatial frequency compared to satellite instrumentation.

### 1. Near-Surface Temperature

The sea-surface temperature has been measured during Superflux (cf. Thomas, 1981) using a PRT-5 passive infrared radiometer which is commercially available. This instrument is similar in character to the satellite infrared sensors and subject to the same considerations.

The near-surface vertical temperature structure has been measured (cf. Leonard, et al., 1979, Leonard, 1980) using the water Raman (O-H stretch) technique. Present accuracy is ±1°C to ±3°C using the 500 nm excitation line from a dye laser operating in a controlled laboratory tank environment. Depth capability is limited to 1 to 2 optical attenuation depths, range-gated at 2 m. The ultimate sensitivity of this technique should be substantially better than ±1°C for cases in which the surface conditions are well defined. The resolution depends on the differential circular depolarization caused by the monomer and polymer species. The accuracy with which a measurement can be made is determined both by system noise considerations and by depolarization effects caused by particulates in the water column. A complementary technique, described by Hirschberg,

et al., 1977, uses Brillouin photon-phonon scattering to provide a measure of the local sound speed in the water as a function of depth. Both methods provide information about the vertical distributions of temperature and salinity.

2. Sea-Surface Salinity

Using an L-band passive microwave radiometer in conjunction with the sea-surface temperature measurement from the PRT-5, measurements have been made of the sea-surface salinity to an accuracy of better than $\pm 1^{o}/oo$ (cf. Kendall, 1981). These measurements are of sufficient accuracy to delineate the plume structure in the Chesapeake Bay and could delineate oceanic fronts with similar salinity discontinuities.

3. Horizontal Distribution of Chlorophyll

The airborne Ocean Color Scanner (OCS), the forerunner to the Nimbus-7 CZCS (cf. Kim et al., 1980), is a passive multispectral radiometer which is designed with ten bands in the visible and infrared portion of the spectrum. Operating from a Lear Jet during Superflux III (cf. Thomas, 1981), this unit exhibited the capability of tracking a feature over a matter of hours, thus extending the period of operations beyond those for a satellite. Using algorithms similar to those developed by Smith and Baker, 1982, and by Gordon , et al., 1980, these data can be used to display the spatial patterns of chlorophyll and of suspended sediment load. The Multichannel Ocean Color Scanner (MOCS) and the Test Bed Multichannel Scanner (TBAMS) are similar instruments, differing in resolution and aerial coverage. The MOCS has 20 bands, 15 nm wide in the visible and near infrared and can be flown both at high and low altitude. The TBAMS was flown only at high altitude, as was the OCS during Superflux II (cf. Thomas, 1981).

4. Vertical Distributions of Chlorophyll

The versions of oceanic LIDAR presently in use (cf. Jarrett, et al., 1979, Leonard, et al., 1979, Bristow, et al., 1980, Hoge and Swift, 1981, and Jarrett, et al., 1981) are active instruments which have the capability of measuring the vertical temperature structure and the vertical distribution of the fluorescence from chlorophyll and other pigments over the upper 1 to 2 optical attenuation depths by range-gating the return signal. These instruments use a pulsed laser source which transmits either a single- or a multiple-wavelength beam in the visible wavelength region from 450 nm to 510 nm. Present capability of the Airborne Oceanic Lidar (AOL) permits range-gating at 2 1/2 m intervals using a 20 ns laser pulse (cf. Hoge and Swift, 1981). The fluorescence from phycoerythrin at 585 nm and from chlorophyll at 685 nm can presently be estimated to within $\pm 25\%$ using this technique; however the penetration depth at 685 nm is less than one-fourth the depth of the deep chlorophyll maximum.

## C. SHIPBOARD MEASUREMENTS

Many of the physical and biological measurements of interest are presently being made from shipboard instrumentation operating either on station or underway. Extensive use can be made of these techniques in any future field programs as fundamental scientific data and as surface truth and calibration data for the remote measurements.

### 1. Temperature and Salinity

The vertical profiles of temperature and salinity are presently obtained using expendable Bathythermograph (XBT) and Conductivity, Temperature and Depth (CTD) instrumentation which are available from commercial sources. The commercial units are now capable of resolutions of 0.0005°C and 0.001 mmhos in conductivity. A shipboard LIDAR unit (cf. Leonard, 1980) should provide along-track measurements of the temperature distribution in the upper 2 optical depths using the water Raman technique. Measurements of the salinity may also be available using an additional Brillouin scattering technique.

### 2. Spectral Irradiance

The upwelling and downwelling irradiance can be measured by a multichannel radiometer developed for open ocean work by Smith and Baker, 1982. These measurements, coupled with measurements of the optical beam attenuation coefficient using either a beam transmission device or using a LIDAR instrument to examine the intensity of the Raman return, will define the integrated optical properties of the water column and provide a measure of the dissolved organic matter and of the concentration of suspended particulate matter in the upper water column.

### 3. Biological Sampling

Onboard pumping systems have been used to obtain water samples from several specific depths. These systems provide samples for the measurement of the fluorescence intensity, using a flow-through fluorometer, and provide filtered chlorophyll samples for calibration of the fluorescent measurements. These systems also provide samples for the measurement of the particle size distribution, using a Coulter counter, or other shipboard analytical technique, and for species analysis to determine the composition of the phytoplankton and zooplankton communities. However, pump systems necessarily impose limitations on the number and locations of samples.

Multiple opening-closing nets (cf. Herman and Platt, 1980) have also been used to sample zooplankton communities for calibration of both optical and acoustical instruments. To provide an adequate sample, nets give a coarse vertical distribution of species abundances, integrated over long path lengths.

4. Chemical Properties

The measurement of oxygen, carbon dioxide, and of nitrate, ammonia, and other nutrients is essential to understanding productivity in the water column and the uptake of $CO_2$ by phytoplankton. These measurements can be made continuously with an onboard pumping system, and can be analysed by standard commercially available instrumentation.

## D. TOWED SUBMERSIBLE INSTRUMENTATION

To provide measurements of the along-track two-dimensional (vertical) physical and biological properties of the water column for correlations with two-dimensional (horizontal) surface images of ocean color provided by an ocean color scanner, a towed submersible must be used that has the capability of acquiring measurements in the region between the surface and a suitable depth below the seasonal thermocline. These measurements should be made in concert with images obtained from the ocean color scanner, with measurements of the upper layer dynamics, and with measurements of the properties of the ocean surface, obtained using ships, aircraft, and moored arrays. A number of towed submersibles which may contribute to these measurements are planned or are in operation.

### 1. Batfish

The Batfish vehicle (Herman and Denman, 1977, Denman and Herman, 1978, Herman and Dauphinee 1980) is considered to be the baseline instrument against which we consider future designs. The Batfish is towed along an undulating track 100 m in amplitude, with a wavelength of 500 m, at tow speeds approaching 6 to 8 kn. The instrumentation in the vehicle permits the measurement of the conductivity, temperature, depth, an *in situ* measurement of the fluorescence from phytoplankton, and the number density of particles in the zooplankton size range. An upward looking radiometer measures the downwelling irradiance, from which the spectrally resolved absorption coefficient can be determined, and an uplooking echosounder determines the depth below the surface. A limited suite of instruments can be accommodated with moderate difficulty in changing the instrument complement. The Batfish is operational and requires a crew of 4 to 5 to operate at sea.

### 2. Sea-Mark II

The Sea-Mark II (Holliday and Pieper, 1980) vehicle is under development. It is designed to be towed at approximately 5 kn at constant depth. A multiple discrete-frequency sonar, using 21 frequencies ranging from 0.1 MHz to 10 MHz will be used to categorize zooplankton in size classes ranging from 100 $\mu$m to 3 cm. The instrument is not range-gated, but integrates the return backscatter signal over a range of 5 to 10 m from the source. Using a theoretical model based on the acoustic scattering from liquid spheres, and using the measured target strengths of individual species, the return signal will be analyzed to produce size classifications of the targets encountered. Surface verification will be provided by

shipboard sampling techniques. The capability for optical measurements is not presently incorporated into the design.

### E. MOORED ARRAYS

For the monitoring of regional basins and ocean current systems that exhibit significant long-term as well as short-term variability, the use of moored arrays of sensors will be necessary to provide long time-series measurements of the biological and physical parameters that define the dynamics of the region. Among these are the measurements that reflect both the availability of nutrients and the biological productivity in the water column. The vertical profiles of temperature and of suspended particulate matter, sampled at frequent intervals over a period of months, will yield information on the detailed time sequence in the dynamics of the upper mixed layer particularly when, because of weather or local surface conditions, the region is out of view of a satellite. Monitoring the fluorescence from chlorophyll and other pigments will permit an assessment of biological activity that can be coupled with acoustical measurements of zooplankton to yield long time-series information both on the productivity of the biomass and on the distributions of and the interactions between the phytoplankton and zooplankton communities. These measurements would require a number of moorings, spaced to provide the boundary value data for the region, and would require that such instrumentation be calibrated periodically to maintain a useful scientific return.

The driving design considerations for a moored array are the power consumption and the data handling capability. Power must be internal and sufficient to operate a mooring for periods in excess of six months to provide a useful data stream. The data capability must include provisions for either continuous or periodic transmission of scientific and housekeeping data to shore, and the capability to monitor the mooring in real time from a ship on station. The design of such an array may benefit from the technology developed for a towed submersible. The combination of time series information with data from towed instruments and satellites provides the fourth, temporal, dimension required to develop an adequate picture of the physical/ecological interactions.

## SECTION IV

## SCIENCE REQUIREMENTS FOR IN SITU INSTRUMENTATION

### A. SUBMERSIBLE SYSTEM DESIGN CONSIDERATIONS

To provide vertical profiles of phytoplankton and zooplankton distributions through the water column, from below the seasonal thermocline to the surface, a towed submersible must be constructed which can accommodate both an underwater LIDAR instrument and a multifrequency sonar. This submersible should include instrumentation to measure the salinity and temperature distributions and an upward-looking echosounder or pressure gauge for measuring the vehicle depth.

The submersible should be designed as a modular vehicle capable of accepting new instrumentation with minimum modification to either the vehicle or the supporting systems. The vehicle should be designed for towing at a maximum speed from 5 to 10 kn, either at constant depth or at a constant value of the potential temperature, $\sigma_T$. The option for depth control should be available while underway from onboard the ship.

The hull should be designed for minimum noise generation and maximum stability, with angular excursions not to exceed $1^{\circ}$ from the tow path. The tow cable should be faired to reduce cable strumming and noise generation, and may be instrumented with thermistors. While maximum depth of operation will be 200 m, the shipboard winch should be capable of handling 500 m of cable, and the hull should be designed for maximum depths of 500 m. All components, including the electronics, the structure, and the instruments, should permit maintenance at sea.

#### 1. Data System

The vehicle data system should collect, format, and transmit the data from the onboard sensors to the shipboard system. The design philosophy should optimize this system to accommodate the required data while maintaining a minimum amount of instrumentation in the submersible. The data system should also provide guidance and control to the vehicle.

The shipboard data system should receive data from the submersible, merge this information with navigation and scientific data from other instruments operated from the ship, and provide the capability to support a real-time display of the appropriate data, together with a statistical analysis of the data as required. This system should record the raw data in real time for post-cruise processing. It should also permit flexibility in the sampling of instruments in real time, and provide instrument control as required. Provision should also be made to receive and evaluate satellite-derived data regarding weather and geophysical features derived from CZCS or other images.



PRECEDING PAGE BLANK NOT FILMED

2. Calibration

Provision should be made for at-sea calibration of each of the instruments employed in the submersible or on shipboard. Where possible, these calibrations should be carried out *in situ*, with particular attention being focused on the spectral reflectance, on the fluorescence from chlorophyll and other pigments, and on the number density of suspended particulate matter.

3. Operations

The submersible should be designed to be used as a national oceanographic facility supported by multiagency users in a cooperative mode. As such, the maintenance and operation should require minimum crew training and shipboard operations, and the vehicle handling requirements should permit the vehicle to be deployed from a number of ships in the oceanographic fleet.

## B. OPTICAL INSTRUMENTATION REQUIREMENTS

The optical instrumentation should be designed to examine the vertical distribution of phytoplankton species, temperature, salinity, and water optical properties, from below the seasonal thermocline to the surface, by range-gating the return signal with a vertical resolution of 1 m. The horizontal spacing between samples should be approximately 10 m because of the assumption that horizontal diffusion creates isotropy on scales that are small compared to the length scale for patchiness. This measurement scheme will create a blurring of the microstructure, which will not be resolved.

To accomplish these goals, the light source should be pulsed, with a pulse length of 5 ns and a pulse repetition rate of 10 to 100 Hz. The energy per pulse, and the maximum pulse rate, should be determined as an optimization of the range of the instrument, maximizing the signal-to-noise ratio for the required horizontal spacing, and maximizing the statistical content of the data. The minimum penetration depth should be 2 optical attenuation depths at a wavelength of 500 nm. The instrument should simultaneously look upward and downward from the vehicle, using multiple excitation wavelengths between 440 nm and 510 nm to take advantage of the minimum in the absorption spectrum and the optimum excitation wavelengths for chlorophyll fluorescence, spectral reflectance, and species identification. The return signal should be spectrally resolved to examine the fluorescence bands of phycoerythrin at 585 nm and chlorophyll at 685 nm, to measure the Mie scattering for the detection of particle concentration, and to measure the water Raman band for the estimation of the optical properties of the water column. Such a spectrometer may also be used to examine bioluminescence in the band at 480 nm. The accuracy required for the measurement of chlorophyll concentrations and for the water optical properties should be better than ± 10%.

Temperature and salinity distributions should be measured remotely with a resolution of 0.1°C/m to provide adequate resolution for biologically important fronts. The accuracy required for the measurement of temperature is ± 0.2°C and for the measurement of salinity is ± 0.2°/oo. As an alternative to the remote optical measurement of the temperature profile, thermistors may be incorporated into the cable above and below the towed vehicle.

The phytoplankton size distributions of interest occur in the range of 3 μm to 200 μm. These particles should be detected, and their volume concentrations estimated by the intensity of the Mie backscatter to an accuracy of ± 10%. For calibration, the total volume of the scattering centers should be estimated near the submersible using beam transmission techniques, or by nephelometry, which does not give a measure of particle size distribution. The use of fluorometry and of commercial counters to determine the particle size distribution in a sample pumped from near the surface can provide an adequate shipboard calibration of the remote detection techniques.

## C. ACOUSTICAL INSTRUMENTATION REQUIREMENTS

To maximize the return of scientific data, it is required to have the spatial resolution and spatial coverage of the acoustical instrumentation comparable to that of the LIDAR. To achieve this coverage range-gating is required to a vertical resolution of 1 m, and sufficient signal-to-noise is required to produce a depth penetration for the acoustical instrument comparable to that provided by the LIDAR instrument. Either simultaneous measurements of the phytoplankton and zooplankton populations are required in the same volume, or the measurement of statistically similar volumes must be made for the intercomparison of these populations. The zooplankton of interest lie in the size range from 100 μm to 3 cm, and characteristically have a very low acoustic impedance and hence a very small target strength. To resolve these size ranges, the acoustic frequencies must lie in the range from 0.1 MHz to 10 MHz. Multiple acoustic frequencies are required to determine the size class distribution to an accuracy of ± 10% and to determine the number density in each size class.

## SECTION V

## OPTICAL INSTRUMENT TECHNOLOGY ASSESSMENT

### A. SYSTEM DESCRIPTION AND FUNCTIONAL REQUIREMENTS

#### 1. Background

The use of satellite-borne remote sensing instrumentation for the measurement of the horizontal distributions and abundances of chlorophyll in the oceans has been described by Smith and Baker, 1982 and by Gordon, et al., 1980. These studies have used data from the Nimbus-7 CZCS, illustrated in Figure 4, to measure the distributions of chlorophyll and to analyse the statistical properties of those distributions. The use of aircraft-borne systems, such as the measurements by Bristow, et al., 1980, have increased our knowledge of the spatial and temporal behavior of these distributions and have provided complementary measurements on different spatial and temporal scales which, together with the satellite data, and with data from ships on station, will lead to a better understanding of the distribution and abundances of species.

The remote observations of the physical structure of the water column have used the water-stretch Raman measurements to infer the optical properties of the water column and to infer the temperature with a demonstrated accuracy of $\pm 3^{o}C$ (cf. Leonard, 1980). These measurements have a potential accuracy of $\pm 0.3^{o}C$, demonstrated theoretically by Leonard, et al., 1979. To complement these measurements, Hirschberg, et al., 1977, have developed Brillouin scattering techniques for the measurement of the local sound speed in water, which have a potential accuracy of better than $\pm 0.5^{o}C$ if the salinity is known to within $\pm 0.5^{o}/oo$. These accuracies have not been realized in practice (cf. Hirschberg, et al., 1980). In regions of strong salinity gradient, the use of a combined Raman-Brillouin system may be required; however, in large areas of the open ocean, the salinity gradients are small above the seasonal thermocline and a single point measurement of the salinity, together with occasional vertical profiles of salinity and temperature will be sufficient to describe the vertical physical structure of the water column.

The optical systems required for the <u>in situ</u> measurement of the vertical distributions and abundances of biota must use the spectral reflectance and the fluorescence from a variety of pigments excited at a number of wavelengths and range-gated at 1 m intervals through the water column. At present, no measurement has been made using <u>in situ</u> instrumentation; however analogous measurements have been made from aircraft and to a limited extent from shipboard.

#### 2. Optical Systems

The optical system for a submersible LIDAR must be capable of performing a number of simultaneous measurements on different physical and



PRECEDING PAGE BLANK NOT FILMED

ORIGINAL PAGE IS
OF POOR QUALITY

biological processes to permit the correlation of the biological populations with the physical environment. The measurements of the vertical distribution of temperature and salinity are central to any description of the physical processes in the water column. The techniques of Raman and Brillouin scattering will be explored as possible sources for these measurements.

Raman scattering occurs as an interaction between the incident light field and the thermally excited molecular vibrations in the water. The wavelength of the scattered light is determined by the wavelength of the incident light, shifted by the vibration of the water molecule. Because water occurs in both monomer and polymer forms, having different vibrational frequencies, the Raman scattered light has the spectral distribution shown in Figure 6. This spectrum was obtained from filtered sea water at 23.8°C, using an incident wavelength of 455 nm. The spectrum is bimodal and the temperature is determined by fitting an ideal bimodal distribution to the data and computing the relative intensities of the monomer and polymer peaks which determine this distribution. The relative intensities are weakly dependent on the salinity. A second, more accurate technique, depends on the differential depolarization of the incident light in the Raman band as a function of temperature. This technique (cf. Leonard, et al., 1979) should produce an accuracy of ±0.3°C.

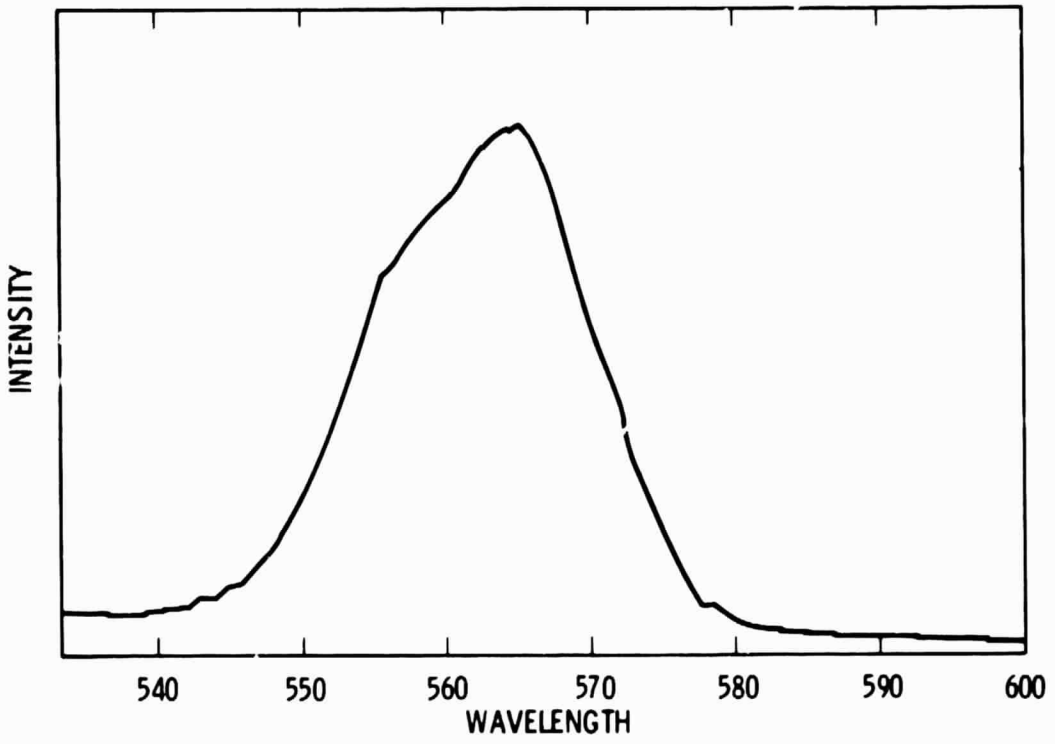


Figure 6. Raman spectrum from filtered sea water at 23.8°C. Laser excitation at 455 nm.

ORIGINAL PAGE IS
OF POOR QUALITY

The integrated intensity of the Raman band is a function only of the intensity of the incident light field and of the absorption of the Raman scattered light in the water column. The integrated signal in this band can then be used to measure the diffuse attenuation coefficient as a function of depth by accounting for the attenuation of the transmitted and Raman scattered beams.

Brillouin scattering occurs as an interaction between the incident light field and ultrasonic waves produced in the water as a result of turbulent processes. The resulting photon-phonon scattering produces a symmetric pair of lines, centered on the incident laser line, and separated from it by a wavelength that is proportional to the sound speed in the water. This phenomenon is illustrated in Figure 7, which was obtained by illuminating distilled water at 20°C with the 514.5 nm line from an Argon-ion laser. The backscattered light was examined using a Fabry-Perot interferometer with a high finesse. The central line in the figure results from Rayleigh and Mie scattering. The symmetric doublet is spaced away from the central line by an amount proportional to the sound speed. For sea water in the normal range of temperature and salinity, this relationship is nearly linear in both temperature and salinity.

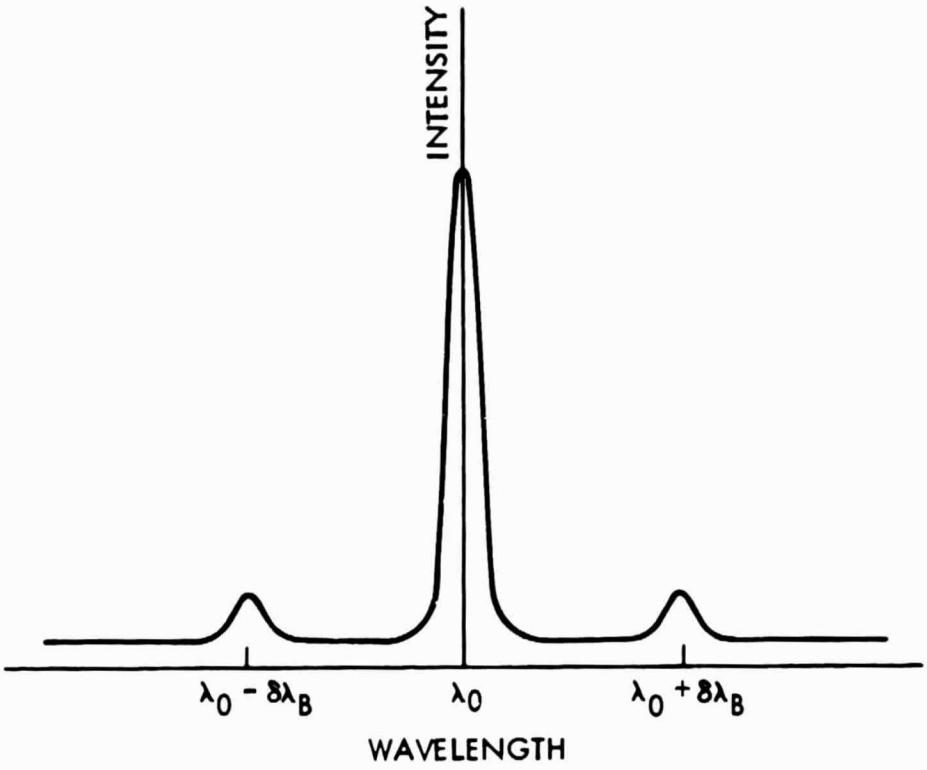


Figure 7. Brillouin triplet in water at 20°C.
Argon-ion laser excitation at 514.5 nm.

The combination of the Raman and Brillouin techniques has the possibility of producing measurements of both the temperature and salinity

ORIGINAL PAGE IS
OF POOR QUALITY

to accuracies of better than ±0.3°C and ±0.5°/oo respectively. There are, however, difficulties in the use of these techniques which require further study. The frequency stability required for the Brillouin measurement may be in excess of that available from a pulsed laser, requiring a hybrid system. Continuing research in this area is expected to resolve the questions of accuracy and of the use of a hybrid technique.

The spectral reflectance from pigmented phytoplankton is a measure both of the particle size through Mie scattering and of the absorption by the pigments illustrated in Figure 2. The absorption is controlled by the state of health of the phytoplankton and by the distribution of species. By illumination at several wavelengths, and observation of the on-wavelength return for each, the taxonomic composition of the phytoplankton can be determined in a manner similar to the measurement of chlorophyll by the CZCS (cf. Gordon, et al., 1980). Algorithms to extract information on the taxonomic composition from spectral reflectance data require additional information including the fluorescence efficiency and fluorescence signatures of the population in question.

By an examination of the fluorescence of chlorophyll *a*, illustrated in Figure 8, and of the fluorescence from other pigments, a measure of the fluorescence efficiency may be obtained. Figure 8 was obtained by illuminating a culture of Dunaliella Tertiolecta in natural concentrations with a XeCl pumped dye laser at 455 nm. The resulting chlorophyll *a* spectrum is centered at 682 nm and has a full width at half maximum of 20 nm. The intensity of the fluorescence is sufficient to permit detection by illuminating the culture with a single pulse from the laser.

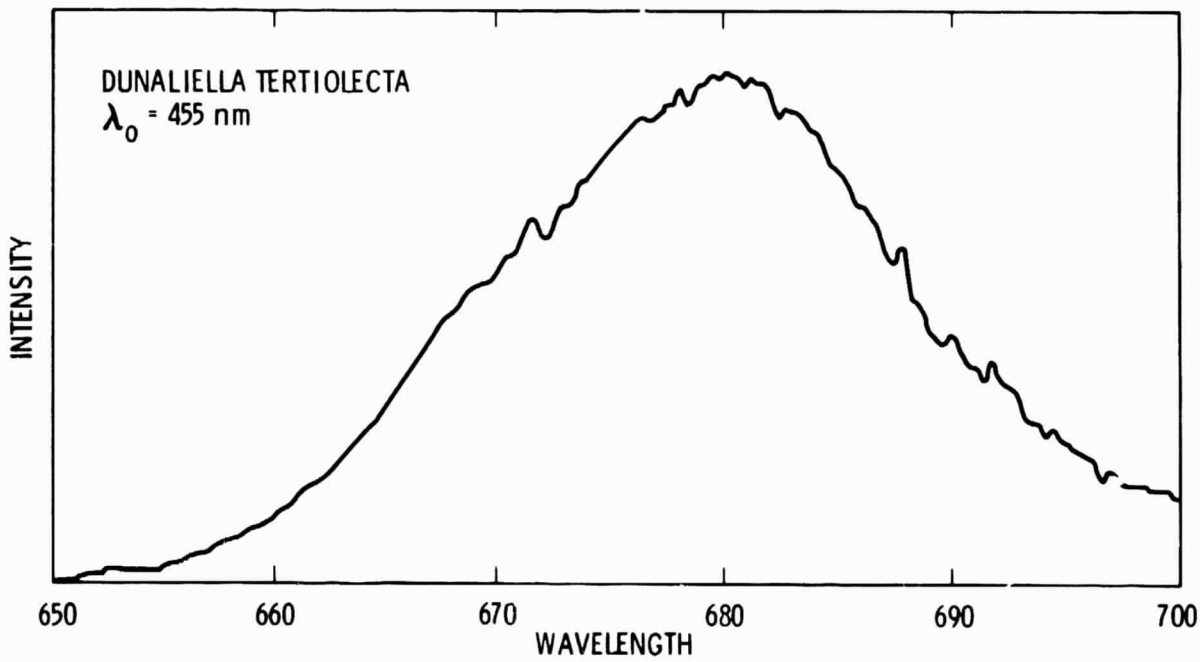


Figure 8. Fluorescence spectrum from Dunaliella Terticlecta. Laser excitation at 455 nm.

Each of these components of the LIDAR signal requires a high resolution spectrometer to examine the data in detail. To achieve a range resolution of 1 m, a laser pulse length of ~ 5 ns is required. This pulse length places restrictions on both the frequency resolution of the receiver and on the data processing system.

## B. TECHNOLOGY ASSESSMENT

The optical measurements of the distributions of particulate matter, pigments and the temperature and salinity, to produce vertical profiles through the upper water column with 1 m vertical resolution and 10 m along track resolution, will require the use of sophisticated laser and optical spectral analysis technology. With the exception of the Brillouin measurement of water temperature, these measurements can be achieved with blue-green pulsed laser sources and range-gated multi-channel analyzer receivers. Measurement configurations employing continuous laser sources, such as a modified commercially available Argon-ion or HeCd laser, may also be considered, although these configurations will be more susceptible to multiple scattering effects which may degrade the spatial resolution.

This section considers the state of technology of blue-green pulsed laser sources and multi-element photodiode arrays which may be used to simultaneously collect the backscattered signals in a large number of spectral resolution elements over the 440 to 700 nm wavelength region. The rapidly developing CCD array technology is not discussed in detail in this section, although it should be stated that these devices are available with readout speeds which are consistent with commercial video requirements, i.e., 10 MHz A/D converter sampling rates.

In this application, the important properties of the potential laser transmitters are output wavelength, reliability and lifetime, and overall electrical efficiency. The importance of a tunable laser source is difficult to assess at the present time, although the capability of using at least two excitation wavelengths is required to characterize both the spectral reflectance and pigment fluorescence features.

### 1. Blue-Green Laser Sources for Oceanic LIDAR

Laser applications in probing sea water either remotely from aircraft or <u>in-situ</u> from a submersible require a laser output wavelength in the blue-green spectral region. For remote sensing from aircraft, or for fluorescence applications with low cross-sections, or low yields, a laser pulse energy of at least 10 mJ is required. Range resolution of 1 m requires a laser pulse width of $\leq$5 ns. For a submersible, optimum pulse energy and repetition rate are 1 to 10 mJ and 10 to 100 Hz, respectively. The capabilities of several laser systems which meet these requirements will be discussed.

The HgBr laser operates at 500 nm. Recent experience has produced an output energy of 1.4 J at 1.7% efficiency with a pulse duration of 100 ns. Whether short duration (5 ns) output from this laser can provide efficient, high energy pulses remains in question. Gas circulation allows high repetition rates; however, the extreme corrosiveness of mercury and bromine at the high temperature required for laser operation may preclude long-life operation. The lifetime for an optimum system is presently under study.

Alexandrite is a solid-state laser which operates in the 730 to 780 nm range. Its output may be mixed in a crystal with the output from a Nd:YAG laser (1060 nm) to produce 450 nm radiation. Both lasers may be flash-lamp pumped and Q-switched for 7 ns output pulse durations. Subsequent mixing should then give a 5 ns output. Repetition rates to 20 Hz are typical of solid-state lasers. Since it is virtually identical to Nd:YAG operation, minimal development would be required. However, this technique would require both the Alexandrite and the Nd:YAG lasers, producing difficult alignment and stability requirements and introducing the possibility of damage to the mixing crystal at higher powers.

The XeCl excimer laser system has a reported output of 5 J/pulse at 1.4% efficiency and recent results have shown greater than 2% efficiency. Spectral bandwidths of <1 GHz are possible, with pulse widths ranging from 4 to 200 ns, and with repetition rates determined by gas recirculation. Gas fill lifetimes of $3 \times 10^6$ shots have been demonstrated. A shifting of the 308 nm XeCl laser radiation directly to the blue-green (459 nm) may be accomplished by a near-resonant stimulated Raman process in Pb vapor. Initial experiments have resulted in energy conversion efficiencies of 40%, with theoretical improvements possible. The heat pipe used in these experiments had a several month lifetime and was highly reliable. Other resonant and non-resonant shifters may be employed to give many wavelengths from 310 to 475 nm. A complete list of the wavelengths available from such sources is given in Table 3.

## TABLE 3. COHERENT LIGHT SOURCES IN VISIBLE AND ULTRAVIOLET SPECTRAL REGIONS

| | WAVELENGTH (nm) | EFFICIENCY (%) | ENERGY (J) | PULSE WIDTH (ns) | REPETITION RATE (Hz) | COMMENTS |
|---|---|---|---|---|---|---|
| Nd: YAG | 1,060 | ≤1 | 0.7 | 9 | 22 | |
| QUANTA RAY | 530 | 0.3 | 0.2 | 7 | 22 | $\lambda_1, \lambda_2, \lambda_3$ are generated by mixing in a crystal. This is a commercial Laser. |
| MODEL DCR-1A | 350 | 0.2 | 0.13 | 5 | 22 | |
| | 270 | 0.07 | 0.05 | 4 | 22 | |
| Nd: YAG Pumped | | | | | | |
| Dye Laser | >530 | 0.1 | 0.075 | 7 | 22 | Tunable, Narrow-Bandwidth Complex System with low efficiency, but available commercially. |
| Frequency Doubled | | | | | | |
| Dye output | >230 | 0.04 | 0.025 | <5 | 22 | |
| Flash Lamp | | | | | | |
| Pumped Dye | | | | | | |
| Doubled output | 960 | 0.5 | 10 | 300 | 0.3 | Low efficiency, short dye lifetime, long pulse widths not appropriate for lidar. Complex systems with low doubling efficiency for UV. |
| (Phase-R model DL-1200 μW) | 220 | 0.01 | | | | |
| Copper Pumped | | | | | | |
| Dye Laser | 550-800 | 0.5 | 0.001 | 20 | 6000 | Good photon conversion but low pulse energy not scalable to high pulse energy. Low doubling efficiency in UV. |
| Metal Vapor | | | | | | |
| Copper | 510-580 | 1 | 0.01 | 10 | >6000 | High repetition rate and low pulse energy. Multiline tunable, except for Cu laser. |
| $Cu^+$ | 248 | <0.01 | $5 \times 10^{-5}$ | | 40 | |
| $Ag^+$ | 318 | <0.01 | $4 \times 10^{-5}$ | | 40 | |
| $Au^+$ | 280 | <0.01 | $6 \times 10^{-5}$ | | 40 | |
| Rare Gas Ion | | | | | | |
| $Ar^+$ | 330-530 | ~0.01 | 20 watts (cw) | | | |
| $Kr^+$ | 330-880 | ~0.01 | 4 watts (cw) | | | |
| Rare Gas Halide Excimer | | | | | | |
| XeCl | 308 | ≥1 | 0.2-5 | 1-100 | 1-1000 | Efficient, scalable, suitable for pumping other media for generation of 450 to 550 nm radiation. |
| Excimer Lasers (Discharge) | | | | | | |
| ArCl | 175 | | | | | |
| ArF | 193-194 | | | | | Many λ's each tunable over 1.0 to 2.0 nm. Narrow spectral width from oscillator-amplifier, 1 kHz repetition rate requires gas recirculation. |
| KrCl | 221-223 | | | | | |
| KrF | 248-249 | 0.1-2 | 0.2-5 | 1-100 | 1-1000 | |
| XeBr | 281-282 | | | | | |
| XeCl | 307-309 | | | | | |
| XeF | 351-353 | | | | | |
| Excimer (XeCl-308 nm) | | | | | | |
| Pumped dye | 320-800 | 0.1-0.2 | 0.12 | 1-100 | 1-1000 | A longer visible wavelength excimer would be more efficient as a dye pump. |
| Frequency doubled | 220-320 | 0.01 | 0.08 | 1-50 | 1-1000 | |

| Raman Shifting of (XeCl-Laser-308 nm) | Stokes Shifts 1st | 2nd | 3rd | | | |
|---|---|---|---|---|---|---|
| $H_2$ | 353 | 414 | 499 | | | Tuning of excimer laser produces tunable Stokes output. |
| $D_2$ | 339 | 377 | 426 | | | |
| $CH_4$ | 338 | 375 | 422 | | | |
| $N_2$ | 337 | 359 | 392 | | | |
| Tl | 405 | | 0.5-0.9 | 2.5-4.5 | 1-100 | 1-100 |
| Pb | 459 | | | | | |
| Ba | 475 | | | | | |
| Bi | 475 | | | | | |



ORIGINAL PAGE IS OF POOR QUALITY

a. Performance Characteristics of Excimer Lasers

The rare-gas halide excimer lasers have undergone considerable development because they provide efficient, high energy laser output at several wavelengths in the ultraviolet. The output wavelengths are: ArF, 193 nm; KrCl, 222 nm; KrF, 248.5 nm; XeBr, 282 nm; XeCl, 308 nm; and XeF, 351 nm. All (except XeF) have fluorescence spectra which indicate an output tuning range of about 1.0 nm. Tunable, high energy, narrow spectral bandwidth output has been demonstrated for ArF, KrF and XeCl in oscillator-amplifier systems.

i. Pulse Width, Energy and Efficiency

For an optimized XeCl system, efficiencies greater than 1% are realized for laser pulse energy greater than one joule. The efficiency is independent of bandwidth because of the homogeneous nature of the bound-free transition. The output pulse width for an optimized XeCl laser may be varied from 5 ns to 100 ns by choosing an appropriate electrical pulse-forming network while maintaining high efficiency.

ii. Spectral Bandwidth and Beam Divergence

For an untuned excimer system, the bandwidth and beam divergence are typically about 0.1 nm and 5 mrad, respectively. Control of these parameters, as well as wavelength is achieved by using an oscillator-amplifier system. For example, an injection-locked KrF laser system has produced 1 J pulses with a spectral bandwidth of 0.001 nm and a divergence of about 100 μrad. The pulse-amplification of a continuous dye laser using a KrF laser has produced 60 mJ pulses with $3 \times 10^{-5}$ nm width and a 50 μrad beam divergence. This narrow bandwidth, low divergence output may be scanned across most of the fluorescence bandwidth (1.0 nm) of the excimer amplifier.

iii. Repetition Rate and Lifetime

Pulse repetition rates of 3 to 5 Hz are possible in a static system. Using laser gas recirculation, repetition rates of 150 to 1000 Hz have been achieved without degrading the efficiency or beam quality of the laser. A system lifetime of $3 \times 10^6$ shots to half-power (at 150 Hz) has been achieved for the XeCl laser. Because these lifetimes are limited by electrode material coating the output windows, improvements in electrode material and in gas recirculation are expected to extend the system lifetime to that of the electrical discharge circuit, ~ $10^8$ charge-discharge cycles.

iv. Laser System Scaling

The rare-gas halide excimer lasers produce a specific output energy of 5 $mJ/cm^3$ and an output energy density of about 0.1 $J/cm^2$. The scaling criteria for these laser systems are reasonably well established, and a design for a specific set of requirements (energy, bandwidth, frequency, pulse width, and repetition rate) can be predicted with a

minimum of development. These systems are the most efficient visible or ultraviolet lasers presently available and hence minimize the requirements for critical resources of size, weight, and power, while minimizing complexity. The optical components used for frequency and bandwidth control are similar to those used for any tunable laser, but the large (~ 1 $cm^2$) aperture of an excimer minimizes alignment requirements.

b. Performance Characteristics of Copper-Halide Lasers

Copper-halide lasers are attractive as possible underwater light sources because they are capable of emitting millijoule pulses with very high pulse repetition rates, thus producing high average power output. The output of a copper-halide laser is at two visible wave lengths, 510.6 nm (green) and 578.2 nm (yellow), with 60% of the power at the green wave length when the laser is operated at maximum pulse energy conditions.

i. Pulse Width, Energy and Efficiency

For both the 510.6 nm and the 578.2 nm output, the pulse width is about 20 ns. The pulse energy, and average power, of a copper-halide laser is a function of the copper-halide vapor density (cf. Pivirotto, 1979). At present, energies of 1 millijoule per pulse are attainable with efficiencies of the order of 0.1%. Using a flowing buffer gas, the laser output pulse energy can be varied. In a typical multiple-pulse laser, buffer gas flow rates of about 0.2 mg/s are used.

ii. Spectral Bandwidth and Beam Divergence

With a stable resonator, the beam divergence half-angle is about 1.5 mrad. With an unstable, confocal, resonator, the beam was estimated to have a divergence half-angle of about 0.1 mrad. The spectrum of the output line exhibits hyperfine structure distributed over several peaks. Etalon selection of a single peak will reduce the rather broad peak to the 0.002 nm width characteristic of a single hyperfine transition.

iii. Repetition Rate and Lifetime

The copper-halide laser is relatively simple and can be built to produce either low or high pulse repetition rates. Extensive work has been done to achieve pulse repetition rates from single shot to 200 pulses per second using double-pulse techniques based on spark-gap technology. To achieve pulse repetition rates from $8 \times 10^3$ to $35 \times 10^3$ pulses per second, hydrogen thyratrons are incorporated into lasers using multiple pulse techniques. The lifetime of these lasers is determined by the consumption rate of the lasing medium and by the electrical components. In a flowing, multiple-pulse laser the consumption rate of copper chloride is about 0.3 gm/h of operation. Lifetimes in excess of $10^8$ shots are presently attainable.

iv. Laser System Scaling

The pulse width can be reduced to as low as 5 ns by proper pulse-discharge circuit design, which should increase the peak pulse intensity and efficiency (cf. Isaev, et al., 1972, Isaev, et al., 1977). Operating the laser at higher pressure with helium should reduce the pulse length and the pulse energy, and produce a smoother pulse intensity distribution with time (cf. Karras, 1980). Reducing the size of the discharge tube, and operating the laser at higher copper-halide densities should decrease the pulse energy, with a shorter pulse length and with a greater peak pulse intensity (cf. Isaev, et al., 1977, Isaev and Lemmerman, 1977).

When a multiple-pulse laser is operated at optimum conditions, the beam diameter should scale with the tube diameter. The maximum theoretical performances of various copper-halide laser configurations are summarized in Table 4.

TABLE 4

COPPER-HALIDE LASER SYSTEM PERFORMANCE

| PULSE REPETITION RATE ($S^{-1}$) | 1 | 10 | $10^2$ | $10^4$ |
|---|---|---|---|---|
| Peak Pulse Intensity ($kW/cm^2$) | 500 | 500 | 33(500) | 75 |
| Pulse Energy (mJ) | 10 | 10 | 0.65(10) | 1.5 |
| Average Power (W) | 0.01 | 0.10 | 0.07(1.0) | 15 |
| Efficiency (%) | 0.01 | 0.05 | 0.08(0.07) | 0.6 |
| Unattended life (h) | 30,000 | 3000 | 300 | 750 |

c. Performance Characteristics of Dye Lasers

Dye laser systems are by far the most advanced of the tunable visible lasers on the commercial market. By using interchangeable dyes, these machines can be tuned through the visible spectrum.

i. Pulse Width, Energy and Efficiency

Dye laser systems use an input pulse from another laser (eg. an excimer), or from a flashlamp. Because the inherent energy transfer efficiency is low, critical alignment is required to achieve optimum pulse energy. Output pulse energies of 25 mJ per pulse are attainable for pulse widths of approximately 5 ns.

ii. Spectral Bandwidth and Beam Divergence

Dye lasers are tunable over 10 nm bandwidths with a given dye; however the efficiency of the dye may vary strongly near the edges of the tuning range. Narrow spectral width operation is attained using a grating and an intracavity etalon, permitting a 0.01 nm to 0.001 nm bandwidth to be obtained, accompanied by a narrow beam divergence.

iii. Repetition Rate and Lifetime

Pulse repetition rates for dye lasers are often restricted by the recirculation time of the dye, and range from 10 to 300 Hz depending on the flow configuration. The lifetime at high power depends on the stability of the dye, and on the nature of any recirculation. Often, dye decomposition limits the operation to a few hours at high power, after which time the laser must be cleaned and fresh dye solution introduced. This will be a serious handicap in an underwater application. Lifetimes of $10^7$ pulses may be an upper bound for many configurations.

iv. Laser System Scaling

The inherent complexity and inefficiency of a two-laser pump-amplifier configuration dominates scaling considerations at all levels.

2. Frequency Shifting

The high output power and high efficiency of excimer lasers allows the use of frequency shifting techniques to obtain an output in the visible part of the spectrum. The simplest of these techniques is stimulated Raman scattering. Because the wavelength shift is fixed using this technique, tuning of the excimer laser also tunes the frequency shifted output, while maintaining the bandwidth. Other possible methods of wavelength shifting include sum or difference frequency mixing with another source, stimulated Brillouin scattering, and optical parametric oscillation.

Stimulated Raman scattering will be discussed because it provides an efficient, stable, passive shifting technique for the conversion of laser radiation from one wavelength to another and may be accomplished with or without pulse compression. This process is a nonlinear interaction involving the third-order nonlinear susceptibility $\chi^3$. A Stokes shifted wave builds up from spontaneous Raman noise through a $\chi^3$ interaction with the pump field. As the first Stokes field builds it depletes the pump field and these two fields mix through a $\chi^3$ interaction, to generate higher orders of Stokes and anti-Stokes waves.

The simplest case of this phenomenon is the nonresonant vibrational Raman shifting using gaseous molecules. For this technique, optimization of the shifting cell's length and pressure can be used to maximize the output for a specific number of Stokes shifts for a collimated monochromatic input wave. Thus, several wavelength regions are accessible using a specific shifting agent, and access to other wavelength regions can be achieved by the use of other agents. Gases such as $H_2$, $D_2$, $CH_4$, and $N_2$ are used at pressures of 1 to 50 atmospheres to provide shifting increments of 4155 $cm^{-1}$, 2916 $cm^{-1}$, and 2326 $cm^{-1}$ respectively. The threshold for stimulated Raman scattering in the visible is about 1 mW for a laser with high mode quality. Once this threshold has been reached for the first Raman shift, additional shifts are parametric with no additional threshold.

Another method of stimulated Raman scattering is the shifting from a near-resonant electronic transition. This method requires a laser whose wavelength is in near coincidence with an electronic transition from the ground state to an excited state which has a strong transition to a third state. This method is of importance because a very large shift is possible in one step and competing processes are minimized thus increasing the overall efficiency. Also, because the near-resonance of the process increases the gain, low pressure operation is possible. This is important because the atomic metal vapors used are contained in heated pipes at temperatures up to 1000°K.

A useful aspect of stimulated Raman scattering is the distinction between the forward and backward directions of Raman scattering caused by Doppler, or other broadening effects which are inhomogeneous to forward scattering, but homogeneous to backward scattering. Thus the backward scattered field accesses a greater portion of the incident field. For scattering in the forward direction the gain coefficient does not depend on pump-laser bandwidth; therefore, efficient broadband scattering is possible. In the backward direction, however, Doppler broadening and pump linewidth affect the ratio of forward to backward gain coefficients. Maximizing the backward gain requires the use of narrow-bandwidth pump lasers. The most important effect of backward Raman scattering is pulse compression. As the backward wave builds in intensity, pump depletion and nonlinear amplification on the leading edge cause a shortening of the input pulse. This type of pulse compressor can be considered as an energy storage laser whose energy is extracted by a short (Stokes-shifted) pulse via $\chi^3$ interaction through the media. Backward stimulated Raman scattering has been shown to be a very efficient means of compressing and extracting the energy of a long input pulse into a short output pulse. This technique may be used in either resonance or nonresonance of the pump with the media.

The excimer lasers whose output wavelengths are closest to the blue-green are XeCl at 308 nm and XeF at 351 nm. Both of these wavelengths would require multiple shifts from $H_2$ (cf. Table 3). However, since computer models indicate that efficient high order stimulated Raman scattering requires a monochromatic beam of high quality, and because for the present application a short output pulse is desired, backward near-

resonant stimulated Raman scattering of an excimer laser should be the best method of shifting and shortening the output pulse because both are accomplished in a single stage.

The XeCl laser has shown high efficiency and high energy when operated with pulse widths of 30 to 100 ns and has demonstrated long gas lifetime (>$3 \times 10^6$ pulses on a single gas fill). To shift and compress the output pulse from a XeCl laser, thallium, lead, or bismuth atomic vapors may be employed (with output wavelengths of 405 nm, 459 nm, and 475 nm, respectively). To produce efficient, narrow bandwidth, diffraction limited output from XeCl, an oscillator-amplifier system is used. The output from this XeCl oscillator-amplifier system is then focused into a heated cell containing the metal vapor. Near the focus, spontaneous backward Raman emission will be amplified and will deplete the pump, producing a short, Stokes-shifted output pulse that is spectrally narrow (~ 0.001 nm). Focusing geometries and metal vapor pressure can be chosen to optimize conversion. If high energies (>1 J) are desired, a stimulated Raman scattering oscillator-amplifier may be preferred, because the focusing of these high energies may give rise to competing processes in the near-resonant stimulated Raman cell.

3. Characteristics of Multielement Diode Arrays

Multiple-element detectors gather signals simultaneously on an array of discrete detector elements. Each element is then scanned in sequence by an electronically-driven shift register at a rate of 10 μs per element. The time to scan the array is determined by the number of elements in the array. An additional 40 μs is used between scans to reset the array. By comparison, the response time of a diode array to a short optical pulse(~ 10 ns) is limited by the RC time constant, which is much less than the scan time.

A dynamic range of 12 bits (4096:1) is accomplished with a low-noise, charge-sensitive preamplifier followed by peak detection in a buffer stage prior to A/D conversion. Signal integration on the elements between scans permits adjustment of exposure times to ensure that maximum use is made of the available dynamic range. Output of the A/D converter is recorded for later signal processing.

While the remaining elements are being read, the previously scanned and cleared ones are again accumulating signal, noise, and background. The maximum scan rate available depends upon the specific device obtained; commercial arrays from Reticon Corp. are available which are self-scanned and operate at 25.6 kHz. These devices may be externally strobed for a data scan instead of using a free-running clock and can easily be operated in a gated fashion at data rates up to 1 MHz. Parallel output arrays in which each element has a separate output line are limited at present to 256 elements.

Photodiode arrays experience noise associated with a dark current caused by leakage discharge of the capacitor in the absence of any optical signal. This noise is temperature dependent and can either be reduced by moderate cooling of the array or may be removed by subtraction. Noise also arises from the electronics involved in reading the array, which may be removed by filtering, sample and hold circuits, or by other techniques. Since this noise appears randomly every time the array is scanned, it cannot be removed by subtraction. An array with a photocathode as the initial optical sensing element also has thermally generated noise from the cathode. This can be reduced by cooling and may also be subtracted out.

Bloom occurs when an intense light signal saturates a detector element and spills over to adjacent detector elements. In addition to severely distorting the signal, it is possible to damage the detector array itself; vidicon detectors are especially susceptible to this process. A strong signal may bloom across the entire array of a vidicon and totally destroy the observed spectrum. Photodiode arrays, such as the Reticon devices, bloom very little or not at all upon saturation of a particular detector element, and are also capable of withstanding repeated saturation without damage. These properties of photodiode arrays are advantageous when observing pulsed return fluorescence signals over some spectral region. Low level signals may be observed without blooming from saturated elements by increasing the gain on an intensified array. Because diode arrays have no inherent gain, gain is provided by the use of an image intensifier (microchannel plate) in front of the array. Using two stages of intensification, variable gain can be provided to values of $10^6$, thus providing photon counting capability. On the next laser shot, the gain may be reduced and the previously saturated high yield return signal examined in detail without being clipped through saturation. As the gain may be controlled electronically, this is an easy approach to implement experimentally.

4. Research Required

Several areas of instrument technology development and research are required to design a towed submersible instrument. Quantitative data on the signal and noise levels to be expected for Brillouin and Raman scattering are needed. Quantitative data on the signal levels to be expected for the spectral reflectance in selected bands, and the optimum bands to be used for the measurement of chlorophyll concentrations are needed. Quantitative data on the signal levels to be expected for the 685 nm chlorophyll *a* fluorescence band are needed for varying water conditions, and investigations into the underwater propagation of laser energy, including wavefront phase and amplitude effects, are needed. A theoretical analysis, substantiated by laboratory measurements, is needed to determine the spectral irradiance (Watts/cm$^2$ per wavenumber) on the entrance aperture of a submersible instrument for the measurement of Raman, Brillouin, turbidity, fluorescence, and backscatter signals. The algorithms required to analyze these data and to produce information on the structure of the physical and biological features in the water are also needed.

Some previous work exists in this area. Leonard, et al., 1979, in a comprehensive paper on Raman scattering measurements of ocean water temperature, provide a data base for the Raman scattering calculations. The measurements of Benedek, et al., 1964, Chiao and Stoicheff, 1964, and of Stegeman, et al., 1970 combine with the theoretical treatments or Mountain, 1966 and of Fabelinskii, 1968 to indicate that a measurement of the Brillouin spectrum will provide accurate temperature and salinity data. Hirschberg, et al., 1980 have used Brillouin scattering to measure temperature, both in the laboratory and in the field. Quantitative information on the signal levels from fluorescence is available from Bristow and Nielsen, 1981, who demonstrate a good signal-to-noise ratio for chlorophyll a fluorescence using a pulsed laser.

## SECTION VI

## ACOUSTICAL INSTRUMENT TECHNOLOGY ASSESSMENT

### A. SYSTEM DESCRIPTION AND FUNCTIONAL REQUIREMENTS

#### 1. Background

The distribution of zooplankton in the euphotic zone of the ocean, and the relationship between the zooplankton populations and the distributions of phytoplankton species are important in understanding the dynamics of the food chain and in understanding the processes which affect the global distribution of carbon and nitrogen. At present, no techniques exist for synoptically measuring the distribution of zooplankton populations from either aircraft or satellites because of the lack of any signature in the electromagnetic spectrum which bears a strong correlation to zooplankton populations. Thus, the measurement of zooplankton populations must continue to be made by shipboard and in situ instruments which sample less than synoptic scales. The traditional sampling techniques using nets and pumps to capture samples for later examination can be augmented by in situ remote measurements of zooplankton populations using acoustical backscatter techniques in which the water column is insonified either by a moored instrument or by an instrument mounted on a towed submersible. This latter approach will provide a vertical along-track profile which can be used to describe the distribution of zooplankton populations and the interrelationship between zooplankton and the physical and biological environment.

Several investigations have studied the distribution of zooplankton species in the water column. Ehrenberg, et al., 1980, have developed a dual coaxial-beam 1.2 MHz instrument for determining the absolute value of the zooplankton target strengths. This instrument utilizes an inner beam which has a spread of $1/3^{o}$ to locate the scatterer near the axis of the outer beam. The $1^{o}$ spread of the outer beam insures that the scatterers that exhibit coincidence are located in a known sound field in the larger beam. Knowledge of the variations of the beam intensity profile with range permits accurate target strength calculations. The signal is corrected for spherical spreading, for attenuation, and for the response of the transducers. Transmitted sound pressure levels of 120 dB produce reverberations at levels of -140 dB from individuals at ranges of 10 m. This is in comparison to background and noise levels of -170 dB. To follow the temporal variability of patches of phytoplankton and zooplankton, these experiments include the use of a 32 thermistor vertical array to measure the temperature structure, the measurement of current, and the measurement of chlorophyll biomass by the use of a moored fluorometer.

Greenblatt, 1981 has used an 87 kHz sonar mounted on the R/V FLIP to study the diurnal migration of zooplankton and the motion of internal waves. This unit used a $1^{o}$ beam mounted below the seasonal thermocline to



PRECEDING PAGE BLANK NOT FILMED

study the migration through the mixed layer. The vertical resolution varied between 3 and 50 m with pulse repetition rates of one per second. These data were correlated with measurements of the temperature distribution, obtained using a thermistor which was lowered through the mixed layer, and with samples obtained from a multiple opening and closing net system.

These results indicate that the structure among zooplankton populations can be detected using scattering from layers of high concentrations, as previously reported by Pieper, 1977. No clearing was noticed which could be attributed to avoidance of the acoustics; however, large variations ($10^{12}$) are noted in scattering cross-sections $\sigma/\pi a^2$, and variations of approximately $10^4$ are noted in equivalent spherical diameter using the Johnson, 1977 liquid sphere model. These results point out the inadequacy of simple models which ignore the details of scattering from dense collections of zooplankton exhibiting large differences in cross-section and shape.

Variations in the scattered intensity in the mixed layer between day and night of 13 dB to 16 dB indicate an early morning downward migration which occurs over a 1 to 2 hour period. The zooplankton exhibit an early evening maxima, in the mixed layer concentrations, with the 4 to 8 mm diameter Euphausiids dominating the scattering late at night and with considerable differences in the clustering between day and night.

Holliday and Pieper, 1980 have studied the distribution of zooplankton size classes in the upper water column using four discrete frequency transducers at 0.5, 1.2, 1.8, and 3.1 MHz. Analysis using the fluid sphere models indicates that this frequency range covers the transition between Rayleigh scattering and geometrical scattering for 1 mm zooplankton. These transducers were mounted as a side-looking sonar on a device designed to be profiled on a wire from a ship on station. Mounted on the instrument is a plankton pump for onboard sampling in the vicinity of the instrument and temperature and conductivity probes for measuring physical variables. Results have been obtained under a number of physical environments.

The data from this instrument has been analyzed using a smoothed version of the Anderson, 1950 liquid sphere model to account for the effects of the plankton carapace. Although significant differences exist between this approach and the physical behavior of zooplankton organisms of interest, the theoretical models are adequate to generate size-class information. These models do not account for either anisotropy or for an ensemble of scatterers in the beam with sizes in the range of 0.1 mm to 10 cm.

A significant amount of theoretical and experimental work has been directed to the understanding of the acoustic backscattering from zooplankton. These studies have demonstrated that the intensity of acoustic backscattering depends strongly on the size and structural shape of the organisms and on the frequency. For the zooplankton of interest in these studies, ranging in size from 0.1 mm to 10 cm, the frequencies of

interest are between 100 kHz and 10 MHz. The interpretation of these data require measured or computed target strength data and the Johnson, 1977 simplification of the Anderson, 1950 liquid sphere model. The target strengths are derived from laboratory experiments (Pieper, Private Communication) in which single animals were suspended by a 20 μm tether and individual target strengths were obtained. In these measurements, 1 mm Copepods were observed at a range of 39 cm using a 10 MHz excitation. It is noted in these experiments that large differences exist between live and preserved species, with live species yielding target strengths that are higher by 6 dB.

2. Acoustical Systems

Two properties of acoustical systems are important in determining their performance: the maximum range, and the range acuity. The maximum range over which a target can be detected is determined by the signal-to-noise ratio of the instrument. The range is frequency dependent both because of differential absorption in the water column, and because practical limitations on transducer design require the beam spread to be a function of frequency. Frequency dependent effects can be removed from the data during processing. The signal-to-noise ratio for detection of acoustical backscattered energy depends on the transmitted energy, on the receiver sensitivity, and on the acoustic scattering cross-section of the organisms under study. For an optimum receiver, an improvement in the signal-to-noise ratio requires an improvement in the transmitted energy which is the product of the pulse duration and the pulse amplitude, and is limited by the nonlinear physical properties of the water column. The use of a linear frequency-modulated sonar, based on the principles of chirp radar, will permit a substantial enhancement of the transmitted energy, over that available using a short duration single-frequency ping system, by increasing the duration of the transmitted signal while maintaining the ability to time-gate the return signal, and to resolve the range to the desired 1 m depth increment. Uncorrelated background noise remains constant for a linear frequency-modulated system and establishes the minimum detectable energy for correlated scatterers and volume reverberation alike.

The range resolution of an acoustic signal is proportional to the reciprocal of the bandwidth of the transmitted signal. For a constant frequency system, the bandwidth is the reciprocal of the pulse length, hence a range resolution of 1 m requires a pulse duration of no more than 0.67 ms. The chirp instrument uses pulse compression techniques to permit the construction of a transmitted signal that exhibits a bandwidth appropriate for the range acuity desired, while extending the time for transmission. This is achieved by the use of a low bandwidth linear frequency modulation superposed on a high frequency signal, permitting an arbitrary pulse duration at fixed bandwidth. For such an instrument the transmitted power increases as the pulse duration while the bandwidth, and hence the range acuity, remain fixed. This may be considered as a continuous time series of single-frequency pulses, each of an appropriate length determined by the ability to distinguish the frequency band in question, and each centered at an ever increasing frequency within the

ORIGINAL PAGE IS
OF POOR QUALITY

limited band of the chirp as illustrated in Figure 9. Thus, for a chirp centered at 500 kHz, with a 3 kHz chirp bandwidth, spanning a time of 300 ms, the transmitted energy is 1000 times that for a single frequency system with a duration of 0.3 ms. The 3 kHz bandwidth is small compared to the minimum frequency of interest in these studies, and variations of ±1.5 kHz are not expected to contribute to uncertainty in size-class definition within the errors which exist in the theory.

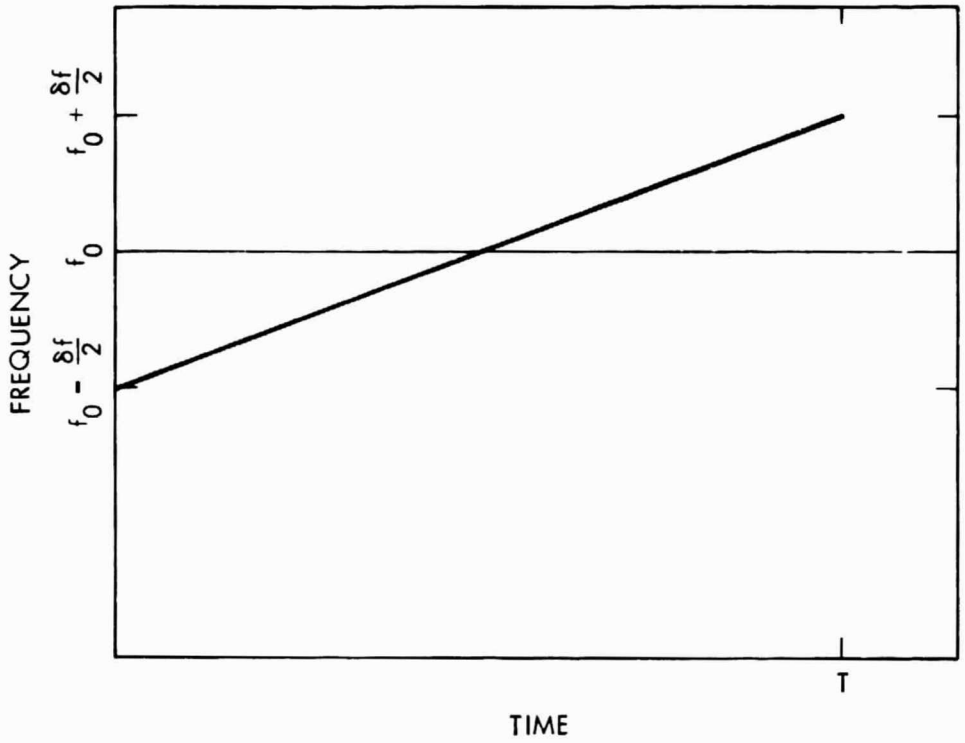


Figure 9. The chirp sonar transmitted signal at frequency $f_o$.

To permit a direct comparison with proposed optical measurements of the structure of the phytoplankton populations, and of the physical structure in the water column, acoustical techniques should insonify a volume that is coincident with or statistically similar to the volume illuminated using optical techniques. This demands a range away from the towed vehicle that coincides with the optical penetration depth expected from the LIDAR instrument, and an insonified volume which is undisturbed by the vehicle and by the tow cable. The sonar should be designed to have a narrow beam configuration with range-gate capability sufficient to produce a 1 m range resolution from a towed submersible. The frequency should span the range from 0.1 to 10 MHz, and be divided into a finite number of discrete bands. These frequencies should be chosen by consideration of the liquid sphere scattering model as a guide to the regions of maximum sensitivity of the organisms under consideration. The information to be recorded should consist of amplitude and time of arrival. It is expected that scattering from multiple organisms in the insonified volume will preclude the use of phase information for species identification.

## B. TECHNOLOGY ASSESSMENT

For remote measurements of zooplankton species through a water column, multiple frequency sonar systems are required which are capable of range acuity with a resolution of 1 m or better and sufficient signal-to-noise to accurately measure these populations at ranges equivalent to two to three optical depths (> 50 m) in clear water. These units should be capable of measurements of acoustic backscatter energy throughout the water column from a vehicle towed at speeds up to 10 kn. The shipboard data handling system should be sufficient to support real-time processing. The development of theoretical models should proceed in parallel with the development of the technology.

The technology discussed here will include the present system of multiple discrete-frequency sonar, and a proposed linear frequency-modulated sonar. The theoretical modeling required to analyze these data will be discussed in the light of existing theory and of extensions of that theory.

### 1. Multiple Discrete-Frequency Sonar

Range resolution for a pulsed sonar is inversely proportional to the duration of transmission, while signal energy and the resultant signal-to-noise performance is proportional to the duration of transmission. The spectral content of a pulse burst is neither uniform nor bounded to a narrow frequency range. Often it is determined by the self-resonance properties of the sonar transducer itself. The result is a suboptimal spread of time domain energy. Since time domain and frequency domain representations are related by a Fourier transform, the best resolution obtainable for a fixed bandwidth pulse system can be achieved by envelope shaping the tone burst by a sin(t)/t response.

A multiple discrete-frequency sonar array is presently under development by Pieper and Holliday which consists of a submersible containing 21 discrete transducers which are tuned independently to cover the frequency range from 100 kHz to 7 MHz. The frequency of each transducer is chosen such that harmonics do not compete with other transducers. The ultimate range and sensitivity remains to be demonstrated for this instrument. Because the pulse has a maximum time-bandwidth product of unity, the projected energy per pulse, and the absorption in the water column as a function of frequency limits the maximum range. Based on a target strength of -120 dB for 1 mm Copepods, the return is expected to be limited to a range of less than 8 m at 7 MHz. The pulse duration for each transducer is 50 μs, corresponding to a range acuity of approximately 4 cm with a repetition rate of 10/s. The beam divergence angles are 3° to 6° and the signal is averaged over a range of 1 m to 8 m from the transducer. By pulse averaging, the signal-to-noise ratio can be improved at the cost of spatial resolution. Improvement can also be noted by increasing the pulse duration from 50 μs to 300 μs for those cases in which one meter range resolution is required.

This sonar will be mounted on a towed submersible which will operate to a depth of 100 m at tow speeds between 4 and 8 kn. This vehicle will carry a 100 kHz uplooking and downlooking sonar for bottom and surface following, a pressure transducer for depth, and thermistors to monitor the temperature environment. An onboard pump will provide a zooplankton sample along-track through a hose to the ship. This sample will be used to study the relative abundances of zooplankton and the abundances of chlorophyll biomass using a shipboard fluorometer.

2. Frequency-Modulated Sonar

The simplest time delay spectrometry (TDS or chirp) system allows two modes of operation. In the first mode, a tracking filter isolates signals which have a constant time delay relative to the moment of transmission and displays the frequency spectrum of that block of time delayed signals. The second mode isolates signal components having a constant frequency content and displays the time delay spectrum of signals occupying that frequency band.

Time delay spectrometry measures both the time domain and frequency domain properties of signals passing through a propagating medium, such as sound in water. The time domain property is complex, with an inphase and a quadrature component. The magnitude of this complex time domain response is proportional to instantaneous total energy density. The phase of this complex time domain response is related to the instantaneous partitioning of signal energy density between its potential and kinetic energy forms. Thus, the form of time domain data made possible by this technique differs from the conventional impulse response, which is the inphase component of the time domain measurement and is related principally to the potential energy density.

The frequency is also complex, with an amplitude and phase. The amplitude is related directly to the conventional power spectral density. For the measurement of zooplankton, the logarithmic amplitude, time delayed relative to the moment of transmission, the energy-time measurement, and the logarithmic frequency spectrum for a given time delay between transmission and reception of sound energy can be used.

In addition to the ease with which frequency domain and time domain measurements may be made, time delay spectrometry also offers technical advantages over more conventional techniques. One advantage is an increased processing gain relative to impulse or pulse measurements. This results because this technique utilizes a spread spectrum in which signal energy is uniformly distributed over a predetermined bandwidth for insonication, and return signals are despread to a much narrower bandwidth, depending on the measurement. The processing gain, expressed as the product of transmit duration and the spread bandwidth, is the time-bandwidth product. Time-bandwidth products of 1000 for underwater applications provide signal-to-noise improvements of 30 dB over pulse systems having the same peak radiating power.

The control of spectrum bandwidth, and the resulting time and frequency domain resolution are an advantage of time delay spectrometry over conventional pulse systems. The system bandwidth is synthesized utilizing signals which bound and define signal energy in the frequency domain. Time domain results are computed from frequency domain measurements. This allows the measurement of noncausal time domain properties. The time domain response includes an optimal resolution since it is computed from a controlled frequency spectrum; the noncausality arises because the computed range time is not the clock time of the sweep.

Frequency spectrum pre-whitening may be achieved for correcting frequency-dependent absorption in a propagating medium. When propagation loss increases with frequency, time domain pulse waveshapes become smoothed and spread unless corrections are made by proper choice of the frequency sweep.

3. Modeling

The target strength is proportional to the logarithm of the backscattering cross section, which can be evaluated theoretically only by using a scattering model. The only model widely used is the Anderson, 1950 fluid sphere model with some simplifications introduced by Johnson, 1977. The results of the Anderson, 1950 model are illustrated in Figure 10. The reason for the almost exclusive use of this model is that the sphere is the only geometric figure for which scattering cross sections can be evaluated analytically for each partial wave, with a summation over partial waves. Greenlaw, 1977 measured scattering strengths of individual preserved zooplankton over a range of frequencies. A simple scattering model was a good approximation for euphausiids and sergestid shrimp, but not for copepods, which exhibit a distinctive orientational dependence of the scattering cross section. Systematic deviations from the Anderson model are also noticed for ka > 1. The need for more refined models for acoustic scattering is also stressed in a more recent study (cf. Greenlaw, 1979) on acoustical estimation of zooplankton populations. Consideration of nonspherical scatterers is the major problem of refined models.

Early attempts to treat scattering from a prolate spheroid (cf. Yeh, 1967) by extension of the analytic approach encountered significant numerical complications, as spheroidal wave functions are very awkward to handle. A more natural approach is that of the transition matrix (cf. Waterman, 1969), in which one constructs a matrix transforming from the initial, known incident wave amplitudes to the final, scattered wave amplitudes. Particularly interesting from the point of view of numerical simplicity, efficiency, and accuracy is the method of optimal truncation described by Visscher, 1980. The central idea is to minimize the amount of nonsatisfaction of the given boundary conditions of the problem caused by the finiteness of the truncated basis set. While in the general case the transition matrix can be full of nonvanishing elements, rendering calculations complex and expensive, in the special case of axial symmetry the matrix decomposes into diagonal blocks, greatly simplifying the calculations.

ORIGINAL PAGE IS
OF POOR QUALITY

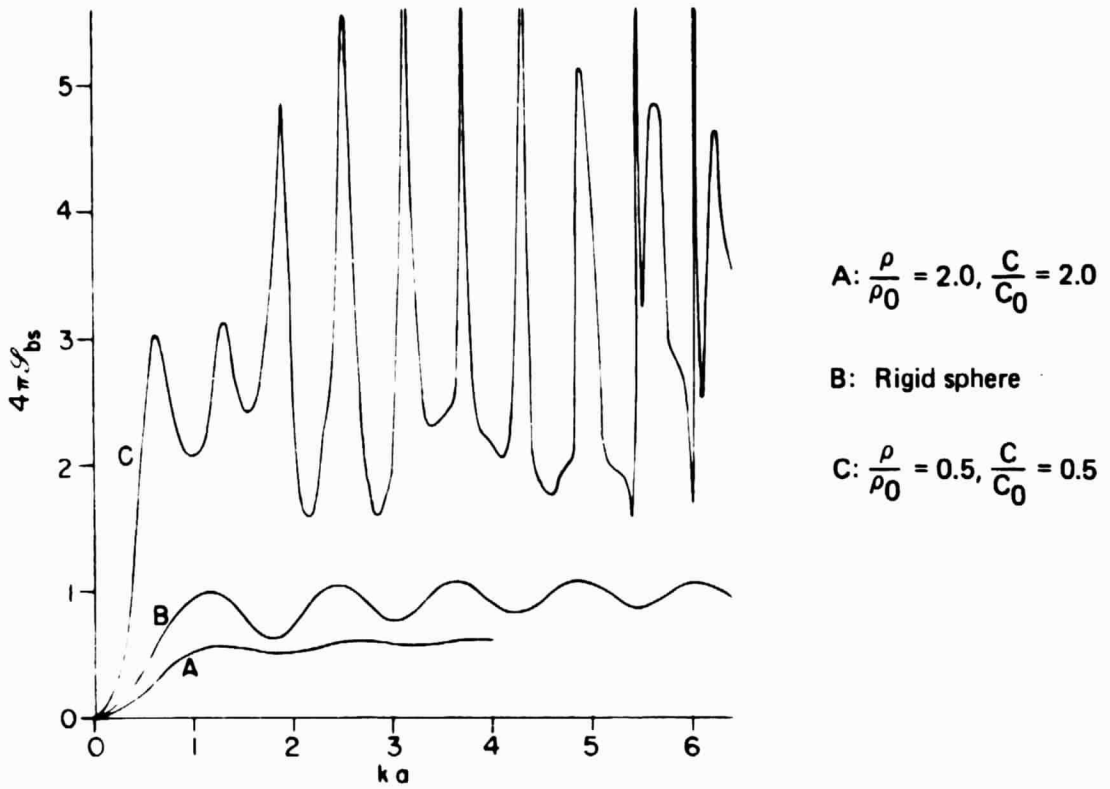


Figure 10. The reflectivity for direct backward scattering of an acoustic wave from a liquid sphere. From Anderson, 1950.

The T-matrix approach has been used to rederive Anderson's results for scattering from a fluid sphere (cf. Jacobi, 1982). The analysis of scattering cross sections for a spheroid, and the dependence of the backscattering cross section on the orientation of the scatterer, has not been performed. The T-matrix approach can also be extended in a natural way to a compound, layered scatterer, though the size of the matrix will increase with the number of scattering layers. Once the scattering cross sections are available for a fluid spheroid, the calculation can be extended to include the effect of an outer elastic shell and/or inner gas bubble, or swimbladder.

While the discussion above refers to a single scatterer, it will be necessary to incorporate the effect of a collection of scatterers, as well as multiple scattering for a high density of scatterers, in this model. A number of such studies are available (cf. Sigelmann and Reid, 1972, Westwater and Cohen, 1973, and Chow and Tien, 1976), where inversion techniques were used to determine droplet and aerosol size distributions in clouds.

## 4. Required Research

The areas of instrument technology development and research required to design a towed submersible instrument include quantitative data which permit the comparison of the chirp technique directly to a ping sonar having the same range acuity or resolution and the same pulse frequency and pulse intensity. This comparison will permit the assessment of these two techniques and the evaluation of the anticipated signal-to-noise ratio enhancement from the chirp sonar. Quantitative data is also required to define the detailed nature of the scattering of acoustic signals from zooplankton populations, including the dependence on size distributions and species types. For this assessment, measurements are required of individual target strengths. Additional modeling is required to extend these measurements to the backscattered signal obtained from collections of individuals of various species. Effects of non-spherical scatters and scattering from multiple targets should be included in these analyses.

PRECEDING PAGE BLANK NOT FILMED

## REFERENCES

Anderson, V. C., 1950, "Sound Scattering from a Fluid Sphere," J. Acoust. Soc. America, 22, 1950, pp. 426-431.

Beers, J. R., Reid, F. M. H., Stewart, G. L., 1975, "Microplankton of the North-Pacific Central Gyre. Population Structures and Abundance," Int. Rev. Gesamten Hydro-Biology, 60, June, 1975, pp. 607-638.

Benedek, G. B., Lastovka, J. B., Fritsch K., Greytak, T., 1964, "Brillouin Scattering in Liquids and Solids Using Low Power Lasers," Journ. Opt. Soc. Amer., 54, 1964, pp. 1284-1285.

Bristow, M., 1978, "Airborne Monitoring of Surface Water Pollutants by Fluorescence Spectroscopy," Remote Sensing of the Environment, 7, Elsevier North-Holland Inc., 1978, pp. 105-127.

Bristow, M., Nielsen, D., Furtek, R., 1979, "A Laser-Fluorosensor Technique for Water Quality Assessment," Proceedings of the 13th International Symposium on Remote Sensing of the Environment, Environmental Research Institute of Michigan, Ann Arbor, Michigan, April, 1979, pp. 397-417.

Bristow, M., Nielsen, D., Bundy, D., Furtek, R., Baker, J., 1980, "Airborne Laser-Fluorsensing of Surface-Water Chlorophyll a," Ocean Remote Sensing Using Lasers, H. R. Gordon, ed., NOAA Technical Memorandum ERL PMEL-18, May, 1980, pp. 97-174.

Bristow, M., Nielsen, D., 1981, "Remote Monitoring of Organic Carbon in Surface Waters," E. P. A. Project Report No. EPA-600/4-81-001, Las Vegas, Nevada, 1981.

Campbell, J. W., Esaias, W. E., Hypes, W. D., 1981, "Superflux I, II, and III Experiment Designs: Remote Sensing Aspects," Chesapeake Bay Plume Study: Superflux 1980, NASA Conference Pub. 2188, January, 1981, pp. 29-42.

Campbell, J. W., Thomas, J. P., 1981, Chesapeake Bay Plume Study: Superflux 1980, NASA Conference Pub. 2188, January, 1981.

Carder, K. L., ed., 1981, "Oceanic LIDAR," NASA Conference Pub. 2194, Nov., 1980.

Chow, L. C., Tien, C. L., 1976, "Inversion Techniques for Determining the Droplet Size Distribution in Clouds: Numerical Examination," Applied Optics, 15, 1976, p. 378.

Chiao, R. Y., Stoicheff, B. P., 1964, "Brillouin Scattering in Liquids Excited by the He-Ne Maser," J. Opt. Soc. Amer. 54, 1964, pp. 1286-1287.

Cullen, J. J., Eppley, R. W., 1981, "Chlorophyll Maximum Layers of the Southern California Bight and Possible Mechanisms of Their Formation and Maintenance," Oceanol. Acta, 4, 1981, pp. 23-32.

Denman, K. L., Herman, A. W., 1978, "Space-Time Structure of a Continental Shelf Ecosystem Measured by a Towed Porpoising Vehicle," J. Marine Research, 36, No. 4, 1978, pp. 693-714.

Ehrenberg, J. E., Traynor, J. J., Williamson, N. J., 1980, "An Evaluation of Methods for Indirectly Measuring The Mean Acoustic Scattering Cross-Section of Fish," Oceans '80: Proceedings of the Conference on Ocean Engineering, Sept., 1980, pp. 371-375.

Eppley, R. W., Harrison, W. G., Chisholm, S. W., Stewart, E., 1977, "Particulate Organic Matter in Surface Waters off Southern California and Its Relationship to Phytoplankton," J. Marine Research, 35, 1977, pp. 671-696.

Esaias, W. E., 1980, "Remote Sensing of Oceanic Phytoplankton: Present Capabilities and Future Goals," Primary Productivity in the Sea, P.G. Falkowski, ed., Plenum Press, N.Y., 1980, pp. 321-337.

Esaias, W. E., 1981, "Remote Sensing in Biological Oceanography," Oceanus, 24, No. 3, Fall, 1981, pp. 32-38.

Fabelinskii, I. L., 1968, Molecular Scattering of Light, Plenum Press, N.Y., 1968.

Gordon, H. R., 1980, "Irradiance Attenuation Coefficient in a Stratified Ocean: A Local Property of the Medium," Applied Optics, 19, No. 13, July, 1980, pp. 2092-2094.

Gordon, H. R., Clark, D. K., Mueller, J. L., Hovis, W. A., 1980, "Phytoplankton Pigments From the Nimbus-7 Coastal Zone Color Scanner: Comparisons With Surface Measurements," Science, 210, Oct., 1980, pp. 63-66.

Gower, J. F. R., Denman, K. L., Holyer, R. J., 1980, "Phytoplankton Patchiness Indicates the Fluctuation Spectrum of Mesoscale Oceanic Structure," Nature, 288, No. 5787, Nov., 1980, pp. 157-159.

Greenblatt, P., 1981, "Sources of Acoustic Backscattering at 87.5 kHz," J. Acoust. Soc. America, 70, 1981, pp. 134-142.

Greenlaw, C. F., 1977, "Backscattering Spectra of Preserved Zooplankton," J. Acoust. Soc. America, 62, 1977, p. 44.

Greenlaw, C. F., 1979, "Acoustic Estimation of Zooplankton Populations," Limnology and Ocean., 24, 1979, p. 226.

Haury, L. R., McGowan, J. A., Wiebe, P. H., 1978, "Patterns and Processes in the Time-Space Scales of Plankton Distributions," Spatial Pattern in Plankton Communities, J. Steele, ed., Plenum Press, N.Y., NATO Conference Series IV, Marine Science, 3, 1978, pp. 277-327.

Herman, A. W., Denman, K. L., 1977, "Rapid Underway Profiling of Chlorophyll with an In Situ Fluorometer Mounted on a 'Batfish' Vehicle," Deep-Sea Research, 24, No. 4, 1977, pp. 385-397.

Herman, A. W., Dauphinee, T. M., 1980, "Continuous and Rapid Profiling of Zooplankton with an Electronic Counter Mounted on a 'Batfish' Vehicle," Deep-Sea Research, 27, No. 1, 1980, pp. 79-96.

Herman, A. W., Platt, T., 1980, "Meso-Scale Spatial Distribution of Plankton: Co-Evolution of Concepts and Instrumentation," Oceanography: The Past, M. Sears, D. Merriman, eds., Springer-Verlag, N.Y., 1980, pp. 204-225.

Herman, A. W., Mitchell, M. R., 1981, "Counting and Identifying Copepod Species with an In Situ Electronic Zooplankton Counter," Submitted to: Deep-Sea Research, 1981.

Hirschberg, J. G., Wouters, A. W., Byrne, J. D., 1977, "Laser Application to Measure Vertical Sea Temperature and Turbidity: Field Test Phase," NASA CR-154623, Dec., 1977.

Hirschberg, J. C., Wouters, A. W., Byrne, J. D., 1980, "Ocean Parameters Using the Brillouin Effect," Ocean Remote Sensing Using Lasers, NOAA Technical Memorandum ERL PMEL-18, H. R. Gordon, ed., 1980.

Holliday, D. V., Pieper, R. E., 1980, "Volume Scattering Strengths and Zooplankton Distributions at Acoustic Frequencies Between 0.5 and 3MHz," J. Acoustical Soc. Am., 67, Jan., 1980, pp. 135-146.

Hoge, F. E., Swift, R. N., 1981, "Application of the NASA Airborne Oceanographic LIDAR to the Mapping of Chlorophyll and Other Organic Pigments," Chesapeake Bay Plume Study: Superflux 1980, NASA Conference Pub. 2188, January, 1981, pp. 349-374.

Hovis, W. A., Clark, D. K., Anderson, F., Austin, R. W., Wilson, W. H., Baker, E. T., Ball, D., Gordon, H. R., Mueller, J. L., El-Sayed, S. Z., Sturm, B., Wrigley, R. C., Yentsch, C. S., 1980, "Nimbus-7 Coastal Zone Color Scanner: System Description and Initial Imagery," Science, 210, Oct., 1980, pp. 60-63.

Isaev, A. A., Kazaryan, M. A., Petrash, G. G., 1972, "Effective Pulsed Copper-Vapor Laser with High Average Generation Power," JETP Letters, 16, No. 1, July, 1972, p. 27.

Isaev, A. A., Kazaryan, M. A., Petrash, G. G., Rautian, S. G. and Shalagin, A. M., 1977, "Shaping of the Output Beam in a Pulsed Gas Laser with an Unstable Resonator," Sov. J. Quantum Electronics, 7, No. 6, June, 1977, p. 746.

Isaev, A. A., Lemmerman, G. Y., 1977, "Investigation of a Copper-Vapor Pulsed Laser at Elevated Powers," Sov. J. Quantum Electronics, 7, No. 7, July 1977, p. 799.

Jacobi, N., 1982, "Scattering from a Fluid Sphere Revisited via a Transition Matrix Approach," J. Acoust. Soc. Am. Suppl. 1, 71, Spring 1982, p. S67.

Jarrett, O., Brown, Jr., C. A., Campbell, J. W., Houghton, W. M., Poole, L. R., 1979, Proceedings of the 13th International Symposium on Remote sensing of the Environment, Environmental Research Institute of Michigan, Ann Arbor, Michigan, April, 1979.

Jarrett, O., Esaias, W. E., Brown, C. A., Pritchard, E. B., 1981, "Analysis of ALOPE Data from Superflux," Chesapeake Bay Plume Study: Superflux 1980, NASA Conference Pub. 2188, January, 1981, pp. 405-416.

Johnson, R. K., 1977, "Sound Scattering from a Fluid Sphere Revisited," J. Acoust. Soc. America, 61, 1977, pp. 375-377.

Karras, T. W., 1980, "Variation of Pulse Width in Copper-Vapor Lasers," Proceedings of the International Conference on Lasers '80, New Orleans, December, 1980, to be published.

Kendall, B. M., 1981, "Remote Sensing of the Chesapeake Bay Plume Salinity Via Microwave Radiometry," Chesapeake Bay Plume Study: Superflux 1980, NASA Conference Pub. 2188, January, 1981, pp. 131-140.

Kim, H. H., McClain, C. R., Blaine, L. R., Hart, W. D., Atkinson, L. P., Yoder, J. A., 1980, "Ocean Chlorophyll Studies From a U-2 Aircraft Platform," J. Geophysical Research, 85, No. C7, July, 1980, pp. 3982-3990.

Leonard, D. A., Caputo, B., Hoge, F. E., 1979, "Remote Sensing of Subsurface Water Temperature by Raman Scattering," Applied Optics. 18, No. 11, June, 1979, pp. 1732-1745.

Leonard, D. A., 1980, "Experimental Field Measurements of Subsurface Water by Raman Spectroscopy," Ocean Remote Sensing Using Lasers, H. R. Gordon, ed., NOAA Technical Memorandum ERL PMEL-18, May, 1980, pp. 45-74.

Mountain, R. O., 1966, "Thermal Relaxation and Brillouin Scattering in Liquids," Journal of Res., N.B.S., 70A, 1966, pp. 207-220.

NASA, 1980, "NASA Oceanic Processes Program," NASA Technical Memorandum, TM-80233, July, 1980.

O'Brien, J. J., 1981, "The Future for Satellite-Derived Surface Winds," Oceanus, 24, No. 3, Fall, 1981, pp. 27-31.

Pieper, R. E., 1977, "Some Comparisons Between Oceanographic Measurements and High Frequency Scattering of Underwater Sound," Oceanic Sound Scattering Prediction, N. R. Andersen, B. J. Zahuranic, eds., Plenum Press, 1977, pp. 667-675.

Pivirotto, T. J., 1979, "Convection Control of the Copper-Halide Vapor Density in a Copper Vapor Laser," Proceedings of the International Conference on Lasers '79, Orlando, Florida, December 1979, p. 315.

Pugh, P. R., 1978, "The Application of Particle Counting to an Understanding of the Small-Scale Distribution of Plankton," Spatial Pattern in Plankton Communities, J. Steele, ed., Plenum Press, N.Y., NATO Conference Series IV, Marine Science, 3, 1978, pp. 111-129.

Sigelman, R. A., Reid, J. M., 1973, "Analysis and Measurement of Ultrasound Backscattering from an Ensemble of Scatterers Excited by Sine-Wave Bursts," J. Acoust. Soc. America, 53, 1973, p. 1351.

Simpson, J. J., Dickey, T. D., 1981, "The Relationship Between Downward Irradiance and Upper Ocean Structure," J. Physical Oceanography, 11, No. 3, March, 1981, pp. 309-323.

Smith, R. C., 1981, "Remote Sensing and Depth Distribution of Ocean Chlorophyll," Marine Ecology Progress Series, 5, August, 1981, pp. 359-361.

Smith, R. C., Baker, K. S., 1981, "Optical Properties of the Clearest Natural Waters," Applied Optics, 20, No. 2, January, 1981, pp. 177-184.

Smith, R. C., Baker, K. S., 1982, "Oceanic Chlorophyll Concentrations as Determined by Satellite (Nimbus-7 Coastal Zone Color Scanner) Marine Biology," 1982, to be published.

Smith, R. C., Eppley, R. W., Baker, K. S., 1982, "Correlation of Primary Production as Measured Aboard Ship in Southern California Coastal Waters and as Estimated from Satellite Chlorophyll Images," Marine Biology, 1982, to be published.

Steele, J. H., 1978, "Some Comments on Plankton Patches," Spatial Pattern in Plankton Communities, J. Steele, ed., Plenum Press, N.Y., NATO Conference Series IV, Marine Science, 3, 1978, pp. 1-20.

Stegeman, G. I. A., Gornall, W. S., Volterra, V., Stoecheff, B, P., 1970, "Brillouin Scattering and Dispersion and Attenuation of Hypersonic Thermal Waves in Liquid Carbon Tetrachloride," Journ. Accoustical Soc. of Amer. 49, 1970, pp. 979-993.

Stewart, R. H., 1981, "Satellite Oceanography: The Instruments," Oceanus, 24, No. 3, Fall, 1981, pp. 66-74.

Thomas, J. P., 1981, "Superflux I, II, and III Experiment Designs: Water Sampling and Analysis," Chesapeake Bay Plume Study: Superflux 1980, NASA Conference Pub. 2188, January, 1981, pp. 43-60.

Visscher, W. M., 1980, "A New Way to Calculate Scattering of Acoustic and Elastic Waves. I. Theory Illustrated for Scalar Waves. II. Application to Elastic Waves Scattered from Voids and Fixed Rigid Obstacles," J. Appl. Phys., 51, 1980, p. 825, p. 835.

Vukovich, F. M., Crissman, B. W., 1980, "Some Aspects of Gulf Stream Western Boundary Eddies From Satellite and In Situ Data," J. Physical Oceanography, 10, No. 11, Nov., 1980, pp. 1792-1813.

Waterman, P. C., 1969, "New Formulation of Acoustic Scattering," J. Acoust. Soc. America, 45, 1969, p. 1417.

Westwater, E. R., Cohen, A., 1973, "Application of Bachus-Gilbert Inversion Technique to Determination of Aerosol Size Distributions from Optical Scattering Measurements," Appl. Optics, 12, 1973, p. 1340.

Wilson, W. S., 1981, "Oceanography from Satellites?," Oceanus, 24, No. 3, Fall, 1981, pp. 9-16

Yeh, C., 1967, "Scattering of Acoustic Waves by a Penetrable Prolate Spheroid. I. Liquid Prolate Spheroid," J. Acoust. Soc. America, 42, 1967, p. 518.

Yentsch, C. S., Yentsch, C. M., 1979, "Fluorescence Spectral Signatures: The Characterization of Phytoplankton Populations by the Use of Excitation and Emission Spectra," J. Marine Research, 37, No. 3, 1979, pp. 471-483.

Zaneveld, J. R. V., Spinrad, R. W., 1979, "An Arc-Tangent Model of Irradiance in the Sea," J. Geophysical Research, 85, No. C9, Sept., 1980, pp. 4919-4922.



NASA—JPL—Coml. L.A. Calif